EMISSION CHARACTERISTICS OF TWO AND THREE LEVEL SYSTEMS

A Thesis Submitted to
the Graduate School of Engineering and Sciences of
İzmir Institute of Technology
in Partial Fulfillment of the Requirements for the Degree of

MASTER OF SCIENCE

in Physics

by
Teyfik YILMAZ

July 2022
İZMİR

ACKNOWLEDGMENTS

I would like to thank my supervisor Assoc. Prof. Dr. Özgür Çakır for his invaluable supports.

This work was supported by The Scientific and Technological Research Council of Turkey (TÜBİTAK) with project number 118E994.

ABSTRACT

EMISSION CHARACTERISTICS OF TWO AND THREE LEVEL SYSTEMS

In this thesis, we mainly focus on the two subjects. Firstly, we investigate the spontaneous emission from a V-type three-level atom. We mainly study the influence of quantum interference between the decay processes from the two upper levels to a lower level to which the upper levels are coupled by the same vacuum modes. The effects of quantum interference on the spontaneous emission spectrum are studied. These effects are shown to induce spectral narrowing and a dark line in the spectrum. The influence of the interference on the upper level populations is also examined. It is seen that the upper level populations are not simple exponential decays. In the second part of this study, the fluorescence spectrum of a driven two-level atom is evaluated. Both the resonance and the off-resonance cases, and the weak and the strong coupling regimes are investigated.

ÖZET

İKİ VE ÜÇ SEVİYELİ SİSTEMLERİN IŞIMA ÖZELLİKLERİ

Bu tezde başlıca iki konu incelenmektedir. İlk olarak üç seviyeli sistemlerde kendiliğinden emisyon fenomeni üzerine çalışılmıştır. Özel olarak V tipi sistemlerde iki bozunma süreci arasındaki kuantum girişim etkilerine odaklanılmıştır. Bu bağlamda, girişimin kendiliğinden emisyon spektrumu üzerindeki etkileri gösterilmiştir. Aynı zamanda girişim fenomeninin atomik enerji seviyelerindeki popülasyonlar üzerindeki etkileri de incelenmiştir. İkinci bölümde ise uyarılmış iki seviyeli atomların ışıma özellikleri incelenmektedir. Bu bölümde zayıf ve güçlü eşleşme rejimleri, hem rezonans hem de rezonans dışı durumlar için çalışılmıştır.

TABLE OF CONTENTS

LIST OF FIGURES vi

CHAPTER 1. INTRODUCTION 1

1.1. Atom-Field Interaction Hamiltonian 1

1.2. Interaction Pictures 5

1.3. Wigner-Weisskopf Theory 8

1.3.1. Wigner-Weisskopf (Born-Markov) Approximation 12

1.4. The Damped Two-Level Atom 14

1.5. Power Spectrum of Emitted Light 22

CHAPTER 2. SPONTANEOUS EMISSION FROM A THREE-LEVEL ATOM ... 26

2.1. Theory 26

2.2. Evolution of the Upper-Level Populations 31

2.3. Power Spectrum of Emitted Light 34

CHAPTER 3. FLUORESCENCE SPECTRUM OF A TWO-LEVEL ATOM 40

3.1. Equations of Motion 40

3.2. Resonance Fluorescence 45

3.3. Discussion and Results 49

CHAPTER 4. CONCLUSIONS 53

REFERENCES 54

APPENDIX A. PRINCIPAL PART INTEGRALS 57

LIST OF FIGURES

Figure **Page**

Figure 1.1 Spectrum of the emitted light by an atom interacting with broad-band thermal field with $\bar{n}(0) = 0$ (blue curve), $\bar{n}(0) = 1$ (red curve), and $\bar{n}(0) = 5$ (orange curve). 25

Figure 2.1 Representative scheme of the atomic model considered in this chapter. It represents a three-level atom in V-type configuration in which the two upper levels are coupled by the same vacuum modes to the lower level, respectively. The energy of the level $|3\rangle$ is higher than the energy of the level $|2\rangle$ by $\hbar\delta$. 26

Figure 2.2 Upper level populations in time. Initially populated state is $|3\rangle$, and its population ρ_{33} (red curve) tediously tends to zero. The population of the level $|2\rangle$, ρ_{22} (black curve), which is initially empty first increases due to the transferred population from level $|3\rangle$, and then tends to zero. ($\delta = \Gamma_3$ and $\Gamma_2 = 0.5\Gamma_3$). 32

Figure 2.3 Maximum value of temporary population in level $|2\rangle$ for three different values of δ, $\delta = 0.1\Gamma_3$ (blue curve), $\delta = 0.2\Gamma_3$ (red curve), and $\delta = 0.3\Gamma_3$ (orange curve) ($\Gamma_3 = \Gamma_2$). 33

Figure 2.4 Illustration of the oscillation of the population in level $|2\rangle$ ($\delta = 5\Gamma_3$ and $\Gamma_2 = \Gamma_3$). 33

Figure 2.5 Total upper level population in time for a few different values of δ. $\delta = 0.1\Gamma_3$ (blue curve), $\delta = 0.5\Gamma_3$ (red curve), and $\delta = 2\Gamma_3$ (orange curve) ($\Gamma_3 = \Gamma_2$). 34

Figure 2.6 Schematic representation of the three-level atom considered in this section. The dashed black line is located at the middle of the energy difference of the upper levels. $\left(\delta_k = \omega_k - \frac{1}{2}\left(\omega_3 - \omega_2\right)\right)$. 35

Figure 2.7 Spectrum of the light emitted spontaneously by a three-level atom (blue curve) for $\delta = 0.6\Gamma_3$, and $\Gamma_2 = 0.1\Gamma_3$, and by a two-level atom (red curve) with decay rate Γ_3. 37

Figure 2.8 Dependence of the width of the dark line in the spontaneous emission spectrum of a three-level atom to the decay rate Γ_2. $\delta = \Gamma_3$, and

$\Gamma_2 = 0.5\Gamma_3$ (blue curve), $\Gamma_2 = 0.05\Gamma_3$ (red curve). 38

Figure 2.9 Narrowing of the spectrum by increasing the ratio Γ_2/Γ_3. Blue curve $(\Gamma_2/\Gamma_3 = 0.01)$, red curve $(\Gamma_2/\Gamma_3 = 0.5)$, orange curve $(\Gamma_2/\Gamma_3 = 2)$, and $\delta = \Gamma_3$ 39

Figure 2.10 Spectrum of the emitted light for three different initial conditions: $\alpha(0) = 1, \beta(0) = 0$ (blue curve), $\alpha(0) = 0.5\beta(0)$ (red curve), and $\alpha(0) = \beta(0)$ (orange curve). $(\delta = 2\Gamma_3, \Gamma_2 = \Gamma_3)$ 39

Figure 3.1 Schematic representation of the driven two-level atom. $|2\rangle$ corresponds to the state with higher energy, and ω_0 is the frequency difference between the states $|2\rangle$ and $|1\rangle$. Ω is the Rabi frequency (represents the frequency of the induced transitions) of the external driving field. ω is the frequency of the incident field. 41

Figure 3.2 Resonance fluorescence spectrum of a two-level atom $(\Delta = 0)$. Weak coupling case: $\Omega = \Gamma$ (blue curve). Intermediate coupling case: $\Omega = 3\Gamma$ (red curve). Strong coupling case: $\Omega = 9\Gamma$ (orange curve). 50

Figure 3.3 Fluorescence spectrum of a two-level system in the case of weak coupling and non-resonant excitation $(\Omega = 0.1\Gamma)$. 51

Figure 3.4 Fluorescence spectrum of a two-level atom for non-resonant and resonant cases $(\Omega = \Gamma)$. 52

Figure 3.5 Fluorescence spectrum for a two-level atom in the strong coupling regime $(\Omega = 5\Gamma)$, for the resonant $\Delta = 0$, and off-resonant $\Delta \neq 0$ cases. 52

CHAPTER 1

INTRODUCTION

In the study of the atom-field interactions, the semi-classical theory assumes that the field is classical (Jaynes and Cummings (1963), Pauli (1980)). In many cases this assumption fails to explain experimentally observed results. For example, spontaneous emission can not be adequately explained by the semi-classical theory and the fully quantum mechanical theory is needed (Shore and Knight (1993)). So, if we want a firm treatment of the decay of an atomic excited state in free-space, it is needed to consider the interaction of the atom with the vacuum modes of the universe. In this chapter, we are going to study the interaction of a two-level atom with the quantized radiation field in free-space (Iqbal et al. (1988)).

In the first section of this chapter, the atom-field interaction Hamiltonian in the dipole and the rotating wave-approximations is introduced. In the second section, we introduce the interaction picture which is an intermediate representation between the Schrödinger picture and the Heisenberg picture. Then, the Wigner-Weisskopf theory (Weisskopf and Wigner (1930)), for a comprehensive study of the spontaneous emission, is introduced. The Heisenberg-Langevin method (Boyanovsky and Jasnow (2017)) is more suitable for the calculation of the two-time correlation function $\langle\hat{\sigma}_+(t+\tau)\hat{\sigma}_-(t)\rangle$ which is required to calculate the spectrum of the emitted light. So, in the last section, we calculate the spectrum of the light emitted by a damped two-level atom.

1.1. Atom-Field Interaction Hamiltonian

In the dipole approximation (Rzazewski and Boyd (2004)), the interaction of the single electron atom and the quantized radiation field $\hat{\mathbf{E}}$ can be expressed by the following Hamiltonian:

$$\hat{H} = \hat{H}_A + \hat{H}_F - \hat{\mathbf{d}}.\hat{\mathbf{E}}. \tag{1.1}$$

In the absence of interaction, $\hat{H}_A$ and $\hat{H}_F$ are the energies of the atom and the

field, respectively, and $\hat{\mathbf{d}}$ is the dipole moment operator. The dipole approximation allows us to assume that the field is uniform over the whole atom (Kobe (1982)).

If the set $\{|i\rangle\}$ constitutes a complete set of atomic energy eigenstates, i.e., $\sum_i |i\rangle\langle i| = 1$, then the atomic transition operators can be written as

$$\hat{\sigma}_{ij} = |i\rangle\langle j|. \tag{1.2}$$

The atom energy $\hat{H}_A$ and the dipole moment operator $\hat{\mathbf{d}}$ can be expressed in terms of the atomic transition operators, and it follows from the eigenvalue equation $\hat{H}_A|i\rangle = E_i|i\rangle$ that

$$\hat{H}_A = \sum_i E_i \hat{\sigma}_{ii}. \tag{1.3}$$

Also the dipole moment operator is

$$\hat{\mathbf{d}} = \sum_{i,j} |i\rangle\langle i|\hat{\mathbf{d}}|j\rangle\langle j| = \sum_{i,j} \mathbf{d}_{ij}\hat{\sigma}_{ij}, \tag{1.4}$$

where the factor $\mathbf{d}_{ij} = \langle i|\hat{\mathbf{d}}|j\rangle$ being the dipole moment operator matrix element between states $|i\rangle$ and $|j\rangle$.

The Hamiltonian operator for the free-field can be written in terms of the creation and annihilation operators as

$$\hat{H}_F = \sum_k \hbar\omega_k(\hat{a}_k^\dagger \hat{a}_k + \frac{1}{2}) \tag{1.5}$$

and after dropping the zero-point energy term, it becomes

$$\hat{H}_F = \sum_k \hbar\omega_k \hat{a}_k^\dagger \hat{a}_k \tag{1.6}$$

In the dipole approximation, the electric field operator can be evaluated at the position of the atom (Barnett and Radmore (1997)). For the atom placed at the origin, the electric field operator is

$$\hat{\mathbf{E}} = \sum_k \mathbf{e}_k \mathcal{E}_k (\hat{a}_k + \hat{a}_k^\dagger) \tag{1.7}$$

where $\mathbf{e}_k$ is the unit polarization vector, and $\mathcal{E}_k = (\hbar\omega_k / 2\epsilon_0 V)^{1/2}$.

Now, by substituting Eqs. (1.3), (1.4), (1.6), and (1.7) into Eq. (1.1) we obtain the following Hamiltonian:

$$\hat{H} = \sum_k \hbar\omega_k \hat{a}_k^\dagger \hat{a}_k + \sum_i E_i \hat{\sigma}_{ii} + \hbar \sum_{i,j} \sum_k g_k^{ij} \sigma_{ij} (\hat{a}_k + \hat{a}_k^\dagger), \tag{1.8}$$

where

$$g_k^{ij} = -\frac{\mathbf{d}_{ij}.\mathbf{e}_k \mathcal{E}_k}{\hbar}, \tag{1.9}$$

for convenience, we assume $\mathbf{d}_{ij}$ to be real.

Now, we consider a two-level atom with the excited state $|e\rangle$ and the ground state $|g\rangle$. Then, for $\mathbf{d}_{ij} = \mathbf{d}_{ji} = \mathbf{d}$, we have

$$g_k = g_k^{eg} = g_k^{ge}. \tag{1.10}$$

The Hamiltonian in Eq. (2.8) becomes

$$\hat{H} = \sum_k \hbar\omega_k \hat{a}_k^\dagger \hat{a}_k + (E_e \hat{\sigma}_{ee} + E_g \hat{\sigma}_{gg}) + \hbar \sum_k g_k (\hat{\sigma}_{eg} + \hat{\sigma}_{ge})(\hat{a}_k + \hat{a}_k^\dagger). \tag{1.11}$$

By using $(E_e - E_g) = \hbar\omega_0$ and $\hat{\sigma}_{ee} + \hat{\sigma}_{gg} = 1$, the second term can be written as

$$E_e \hat{\sigma}_{ee} + E_g \hat{\sigma}_{gg} = \frac{1}{2}\hbar\omega_0 (\hat{\sigma}_{ee} - \hat{\sigma}_{gg}) + \frac{1}{2}(E_e + E_g). \tag{1.12}$$

The projectors $|e\rangle\langle e|$, $|e\rangle\langle g|$, $|g\rangle\langle e|$, and $|g\rangle\langle g|$, and their combinations are the only possible operators for our two-level atom. As usual, these operators are used in the form of the Pauli operators

$$\hat{\sigma}_3 = |e\rangle\langle e| - |g\rangle\langle g| \tag{1.13}$$

$$\hat{\sigma}_+ = |e\rangle\langle g| \tag{1.14}$$

$$\hat{\sigma}_- = |g\rangle\langle e|, \tag{1.15}$$

The first operator is a Hermitian operator while the second and the third constitutes a Hermitian conjugate pair such that $\hat{\sigma}_+ = \hat{\sigma}_-^\dagger$, and these operators satisfy the following commutation relations:

$$[\hat{\sigma}_-, \hat{\sigma}_+] = -\hat{\sigma}_3 \tag{1.16}$$

$$[\hat{\sigma}_-, \hat{\sigma}_3] = 2\hat{\sigma}_-. \tag{1.17}$$

In the matrix form, the operators $\hat{\sigma}_3$, $\hat{\sigma}_+$, and $\hat{\sigma}_-$ are given by

$$\hat{\sigma}_3 = \begin{bmatrix} 1 & 0 \\ 0 & -1 \end{bmatrix}, \hat{\sigma}_+ = \begin{bmatrix} 0 & 1 \\ 0 & 0 \end{bmatrix}, \hat{\sigma}_- = \begin{bmatrix} 0 & 0 \\ 1 & 0 \end{bmatrix}. \tag{1.18}$$

The $\hat{\sigma}_3$ operator is the atomic inversion. The $\hat{\sigma}_+$ and $\hat{\sigma}_-$ operators are the atomic transition operators. The $\hat{\sigma}_+$ operator takes the atom from the ground state to the excited state whereas the $\hat{\sigma}_+$ takes the atom from the excited state to the ground state.

By using these operators and ignoring the constant energy term in Eq. (1.12), the Hamiltonian in Eq. (1.11) can be rewritten as

$$\hat{H} = \sum_k \hbar\omega_k \hat{a}_k^\dagger \hat{a}_k + \frac{1}{2}\hbar\omega_0 \hat{\sigma}_3 + \hbar \sum_k g_k(\hat{\sigma}_+ + \hat{\sigma}_-)(\hat{a}_k + \hat{a}_k^\dagger). \tag{1.19}$$

The interaction part in the above equation contains four terms. The term $\hat{\sigma}_+\hat{a}_k$ corresponds to the case in which the atom makes a transition from the ground state to the

excited state whereas a photon of mode k is destroyed. The term $\hat{\sigma}_{-}\hat{a}_k^{\dagger}$ corresponds to the opposite case. For these two cases, the energy is conserved. The term $\hat{\sigma}_{+}\hat{a}_k^{\dagger}$ corresponds to the case in which the atom makes a transition from the ground state to the excited state and a photon is created. In this situation, the system gains energy nearly equal to $2\hbar\omega$. For the term $\hat{\sigma}_{-}\hat{a}_k$, the process is reversed, and the system loses energy, approximately equal to $2\hbar\omega$. These two terms are the energy non-conserving terms. Then, dropping these terms corresponds to the rotating-wave approximation (Irish (2007), Gerry and Knight (2004)). So, the Hamiltonian in Eq. (1.19) becomes

$$\hat{H} = \frac{1}{2}\hbar\omega_0\hat{\sigma}_3 + \sum_k \hbar\omega_k\hat{a}_k^{\dagger}\hat{a}_k + \hbar\sum_k g_k(\hat{\sigma}_{+}\hat{a}_k + \hat{a}_k^{\dagger}\hat{\sigma}_{-}). \tag{1.20}$$

The interaction of a single two-level atom with a multi-mode field is described by the Hamiltonian in eq. (1.20).

1.2. Interaction Pictures

In quantum mechanics, the dynamics of a system is examined by several equivalent pictures, or descriptions. They are connected to each other by unitary transformations. Interaction pictures represent the descriptions between the Schrödinger and the Heisenberg pictures. In the Heisenberg picture, the state is time independent and all the dynamics are contained within the operators. On the other hand, the state evolves while the operators are time independent in the Schrödinger picture. In some of the interaction pictures which are called as the Schrödinger interaction pictures, the dynamics associated with the free evolution is contained within the operators, while evolution arising from the coupling is contained in the state, and vice versa for the pictures known as the Heisenberg interaction pictures. (Barnett and Radmore (1997)).

The unitary transformations connect the Schrödinger interaction pictures to each other. The expectation values of the observables must be independent of the picture in which it is evaluated. For an operator $\hat{A}$, for example, the expectation value in a state $|\psi\rangle$ is given by $\langle\psi|\hat{A}|\psi\rangle$. By the use of an unitary operator $\hat{U}$, the transformation to a

Schrödinger interaction picture is attained. In this picture, while the state is

$$|\psi_1\rangle = \hat{U}|\psi\rangle, \tag{1.21}$$

the operator $\hat{A}$ becomes $\hat{U}\hat{A}\hat{U}^\dagger$. Then, the invariance of the expectation value results from $\hat{U}^\dagger = \hat{U}^{-1}$, that is,

$$\langle\psi_1|\hat{U}\hat{A}\hat{U}^\dagger|\psi_1\rangle = \langle\psi|\hat{U}^\dagger\hat{U}\hat{A}\hat{U}^\dagger\hat{U}|\psi\rangle \tag{1.22}$$

$$= \langle\psi|\hat{U}^{-1}\hat{U}\hat{A}\hat{U}^{-1}\hat{U}|\psi\rangle \tag{1.23}$$

$$= \langle\psi|\hat{A}|\psi\rangle. \tag{1.24}$$

In order to obtain the interaction picture Hamiltanian, we use the Schrödinger equation

$$i\hbar\frac{\partial|\psi\rangle}{\partial t} = \hat{H}|\psi\rangle, \tag{1.25}$$

and the condition that $|\psi_1\rangle$ obeys the transformed Schrödinger equation

$$i\hbar\frac{\partial|\psi_1\rangle}{\partial t} = \hat{\mathcal{V}}|\psi_1\rangle. \tag{1.26}$$

By substituting eq. (1.21) into eq. (1.26), we have

$$i\hbar\left(\dot{\hat{U}}|\psi\rangle + \hat{U}\frac{\partial|\psi\rangle}{\partial t}\right) = i\hbar\dot{\hat{U}}|\psi\rangle + \hat{U}\hat{H}|\psi\rangle = \hat{\mathcal{V}}\hat{U}|\psi\rangle. \tag{1.27}$$

To obtain the above expression we have used eq. (1.25), and from this expression the interaction picture Hamiltonian is

$$\hat{\mathcal{V}} = U\hat{H}U^\dagger + i\hbar\dot{\hat{U}}U^\dagger. \tag{1.28}$$

Now, as an example we transform the Hamiltonian

$$\hat{H} = \frac{1}{2}\hbar\omega_0\hat{\sigma}_3 + \sum_k \hbar\omega_k \hat{a}_k^\dagger \hat{a}_k + \hbar \sum_k g_k(\hat{\sigma}_+ \hat{a}_k + \hat{a}_k^\dagger \hat{\sigma}_-). \tag{1.29}$$

This is the Hamiltonian that we obtain in the previous section, and we want to transform it into a Schrödinger interaction picture in which the interaction picture Hamiltonian does not contain the free evolution term both for the atom and the field. In order to achieve this we use the corresponding unitary transformation:

$$\hat{U} = exp\left\{\frac{i}{\hbar}\left(\frac{1}{2}\hbar\omega_0\hat{\sigma}_3 + \sum_k \hbar\omega_k \hat{a}_k^\dagger \hat{a}_k\right) t\right\}. \tag{1.30}$$

By using the Baker-Hausdorf lemma: for any two operators $\hat{A}$ and $\hat{B}$,

$$e^{\alpha\hat{A}}\hat{B}e^{-\alpha\hat{A}} = \hat{B} + \alpha[\hat{A},\hat{B}] + \frac{\alpha^2}{2}[\hat{A},[\hat{A},\hat{B}]] + ..., \tag{1.31}$$

we can easily see that

$$\hat{U}\hat{a}\hat{U}^\dagger = \hat{a}e^{-i\omega_k t} \tag{1.32}$$

$$\hat{U}\hat{\sigma}_+\hat{U}^\dagger = \hat{\sigma}_+ e^{i\omega_0 t}. \tag{1.33}$$

Now we write the corresponding interaction picture Hamiltonian as follows

$$\hat{\mathcal{V}} = \hbar \sum_k g_k \left(\hat{\sigma}_+ \hat{a}_k e^{-i\Delta_k t} + \hat{a}_k^\dagger \hat{\sigma}_- e^{i\Delta_k t}\right), \tag{1.34}$$

where $\Delta_k = \omega_k - \omega_0$ is the detuning between the atomic transition frequency and the k^{th} mode of the field.

If we consider, now, a Heisenberg interaction picture in which time dependence arising from the coupling is carried by the operators, and for an operator $\hat{A}$ with no explicit

time dependence the equation of motion given by

$$\dot{\hat{A}} = \frac{i}{\hbar}\left[\hat{\mathcal{V}}, \hat{A}\right]. \tag{1.35}$$

In the above equation, $\hat{\mathcal{V}}$ is obtained from eq. (1.28). As mentioned previously, the time dependence is partly contained within the state, too. We will work in the Heisenberg interaction picture later in the subsequent sections.

1.3. Wigner-Weisskopf Theory

For the case of an excited atom in free-space, there are infinitely many modes that it couples. Due to the coupling to the modes, the atom spontaneously and irreversibly decays to a lower energy level. In this case, the dynamics is well described by the Wigner-Weisskopf theory (Stenholm and Suominen (1930)).

Here, we are aiming to solve for the evolution of the atom-field system which is described by the Hamiltonian

$$\hat{H} = \frac{1}{2}\hbar\omega_0\hat{\sigma}_3 + \sum_k \hbar\omega_k\hat{a}_k^\dagger\hat{a}_k + \hbar\sum_k g_k(\hat{\sigma}_+\hat{a}_k + \hat{a}_k^\dagger\hat{\sigma}_-). \tag{1.36}$$

It is convenient to work in the interaction picture. So, the corresponding Schrödinger interaction picture Hamiltanian is given in eq. (1.34):

$$\hat{\mathcal{V}} = \hbar\sum_k g_k\left(\hat{\sigma}_+\hat{a}_k e^{-i\Delta_k t} + \hat{a}_k^\dagger\hat{\sigma}_- e^{i\Delta_k t}\right). \tag{1.37}$$

The initial state vector is

$$|\psi(0)\rangle = |e\rangle \otimes |0\rangle. \tag{1.38}$$

Time evolution of the state vector is governed by the Schrödinger equation:

$$i\hbar\frac{\partial|\psi(t)\rangle}{\partial t} = \hat{\mathcal{V}}|\psi(t)\rangle. \tag{1.39}$$

At time $t > 0$, the state vector can be written as

$$|\psi(t)\rangle = C_1(t)|e\rangle \otimes |0\rangle + \sum_k C_2(t)|g\rangle \otimes |1_k\rangle. \tag{1.40}$$

By substituting the eqs. (1.37) and (1.40) into eq. (1.39), we obtain the equations of the motion for the probability amplitudes

$$\dot{C}_2(t) = -\frac{i}{\hbar}\left(\langle e| \otimes \langle 0|\right)\hat{\mathcal{V}}|\psi(t)\rangle = -i\sum_k g_k e^{-i(\omega_k-\omega_0)t}C_1(t) \tag{1.41}$$

$$\dot{C}_1(t) = -\frac{i}{\hbar}\left(\langle g| \otimes \langle 1_k|\right)\hat{\mathcal{V}}|\psi(t)\rangle = -ig_k e^{i(\omega_k-\omega_0)t}C_2(t). \tag{1.42}$$

By formally integrating the eq. (1.42), we have

$$C_1(t) = -ig_k\int_0^t e^{-i(\omega_k-\omega_0)t'}dt', \tag{1.43}$$

and putting this into eq. (1.41) will yield the following integro-differential equation

$$\dot{C}_2(t) = -\sum_k g_k^2\int_0^t e^{-i(\omega_k-\omega_0)(t-t')}C_2(t'). \tag{1.44}$$

In the case of an excited atom interacting with a single free-space mode, the set of coupled first-order differential equations for the amplitudes, under the assumption that the coupling is weak, so that the initial state population changes very little, will be solved by adopting a perturbative approach. This leads us to end up with the famous Fermi's Golden rule. However, an atom in free-space is an open quantum system in which the atom couples to the continuum of modes. In this case, perturbation approach must be

abandoned. The dynamics is well described by Wigner-Weisskopf theory.

Here, we want to describe the evolution in free-space. The free-space can be imagined to be a cubic cavity of side length L. Then, by taking the boundaries of the cavity to infinity, the sum over a discrete set of modes becomes an integral over a continuum of modes. By using the density of states concept, the number of modes can be counted. For example, the number of modes in a volume d^3k of k-space is given by $\mathcal{D}(\vec{k})d^3k$ where $\mathcal{D}(\vec{k})$ is the density of modes.

The quantization in a cubical box of side length L will impose periodic boundary conditions. In the x-direction, for example, the plane waves must satisfy the condition

$$e^{ik_x x} = e^{ik_x(x+L)}, \tag{1.45}$$

and it follows that

$$k_x = \frac{2\pi}{L} n_x; \quad n_x = 0, \pm 1, \pm 2, ... \tag{1.46}$$

For the y- and z-directions, the same boundary conditions will give

$$k_y = \frac{2\pi}{L} n_y; \quad n_y = 0, \pm 1, \pm 2, ... \tag{1.47}$$

$$k_z = \frac{2\pi}{L} n_z; \quad n_z = 0, \pm 1, \pm 2, ... \tag{1.48}$$

Thus, the discrete set of modes are

$$\mathbf{k} = \frac{2\pi}{L}(n_x, n_y, n_z), \tag{1.49}$$

and a set of integers (n_x, n_y, n_z) specifies a normal mode of the field apart from the

polarization. Then, the density of modes is

$$D(\mathbf{k}) = \frac{1mode}{\left(\frac{2\pi}{L}\right)^3} = \frac{V}{(2\pi)^3}. \tag{1.50}$$

Thus, the summation over the discrete modes can be replaced by an integral as following

$$\sum_k = \int \mathcal{D}(\mathbf{k}) d^3k. \tag{1.51}$$

In spherical coordinates, the volume element d^3k becomes

$$d^3k = k^2 sin\theta d\theta d\phi dk = k^2 d\Omega dk, \tag{1.52}$$

where $d\Omega$ is the element of solid angle. By using the expression $k = \omega_k/c$ the Eq.(1.44) can be transformed into

$$\sum_k = \int \mathcal{D}(\vec{k}) \frac{\omega_k^2}{c^3} d\Omega_k d\omega_k = \int \mathcal{D}(\omega_k) d\Omega_k d\omega_k, \tag{1.53}$$

where $\mathcal{D}(\omega_k)$ is the mode density in frequency in a shell of k-space of radius ω_k/c. Thus, in the continuum limit

$$\dot{C}_2(t) = -\int_0^\infty d\omega_k \mathcal{D}(\omega_k) \left(\int d\Omega_k \sum_\mu g_\mu^2(\mathbf{k}) \right) \int_0^t dt' e^{-i(\omega_k - \omega_0)(t-t')} C_2(t'). \tag{1.54}$$

The summation over μ takes into account the different polarizations of the modes. Thus, the polarization average is defined to be

$$\overline{g^2(\omega_k)} \equiv \int d\Omega_k \sum_\mu g_\mu^2(\mathbf{k}) = \frac{1}{\hbar^2} \left(\frac{\hbar\omega_k}{2\epsilon_0 V} \right) \int d\Omega_k \sum_\mu \left(\mathbf{d}.\mathbf{e}_k \right)^2, \tag{1.55}$$

where

$$\sum_{\mu} \left(\mathbf{d}.\mathbf{e}_k\right)^2 = sin^2(\theta_k) \left(\mathbf{d}\right)^2 . \tag{1.56}$$

Now, we rewrite the eq. (2.44) as

$$\dot{C}_2(t) = -\int_0^{\infty} d\omega_k \overline{g^2(\omega_k)} \mathcal{D}(\omega_k) \int_0^t dt' e^{-i(\omega_k-\omega_0)(t-t')} C_2(t'). \tag{1.57}$$

In obtaining Eq. (1.57) we have assumed that the atomic dipole moment is pointing along the z-direction, and the angle between the wave-vector $\vec{k}$ and the dipole moment is θ_k.

1.3.1. Wigner-Weisskopf (Born-Markov) Approximation

Other than the dipole and the rotating-wave approximations, we have made no approximations, so far. Therefore, the eq. (1.57) is exact up to the dipole and the rotating-wave approximations. A much more essential approximation will be introduced here. Before this, we give two fundamental assumptions that the approximation based on. Firstly, we assume that the coupling is weak so that $C_2(t)$ varies much more slower than ω_0. The other assumption is that the continuum is very broad, and changes very little in time scales that contribute to the integral.

In eq. (1.57), the exponential factor oscillates very fast for all times $t' < t$ due to the broad continuum. Compared to these fast oscillations, $C_2(t')$ varies very slowly. Thus, the end-point value of the integral will dominate, where at $t' = t$. Therefore, we replace $C_2(t')$ by its value at t, that is $C_2(t)$. Since $C_2(t)$ is independent of the integral variable, we take it out of the integral. Then, the only value of C_2 at t contributes to the evolution of $C_2(t)$, it is independent of the whole history. Now, the eq. (1.57) can be written as

$$\dot{C}_2(t) \approx -\left[\int_0^{\infty} d\omega_k \overline{g^2(\omega_k)} \mathcal{D}(\omega_k) \int_0^t dt' e^{-i(\omega_k-\omega_0)(t-t')}\right] C_2(t). \tag{1.58}$$

Again by the same assumption that the continuum is broad so that the exponential factor oscillates very fast compared to the variation of the probability amplitude, then the value of the integral vanishes for $t >> t'$. Therefore, we let the upper limit of the time integral to go to infinity,

$$\dot{C}_2(t) \approx -\left[\int_0^\infty d\omega_k \overline{g^2(\omega_k)}\mathcal{D}(\omega_k)\int_0^\infty d\tau e^{-i(\omega_k-\omega_0)\tau}\right] C_2(t) \tag{1.59}$$

$$\approx -\left[\int_0^\infty d\omega_k \overline{g^2(\omega_k)}\mathcal{D}(\omega_k)\zeta(\omega_k-\omega)\right] C_2(t), \tag{1.60}$$

where

$$\zeta(\omega) \equiv \int_0^\infty e^{-i\omega\tau} d\tau. \tag{1.61}$$

However, this is not a convergent function. In order to ensure that the integral over τ converges, we multiply it by the convergence factor $exp(-\epsilon\tau)$, and take the limit as $\epsilon \to 0^+$ after evaluating the integral. Thus, the integral in eq. (1.61) becomes

$$\zeta(\omega) = \lim_{\epsilon\to\ 0^+}\int_0^\infty e^{-i\omega\tau-\epsilon\tau}d\tau = \lim_{\epsilon\to\ 0^+}\frac{1}{i\omega+\epsilon}. \tag{1.62}$$

Seperating the real and imaginary parts of the function inside the limit yields

$$\zeta(\omega) = \lim_{\epsilon\to\ 0^+}\left[\frac{\epsilon}{\omega^2+\epsilon^2} - i\frac{\omega}{\omega^2+\epsilon^2}\right]. \tag{1.63}$$

By using the eq. (A.6) from the Appendix A, we have

$$\lim_{\epsilon\to\ 0^+}\frac{1}{i\omega+\epsilon} = \pi\delta(\omega) - i\frac{P}{\omega}. \tag{1.64}$$

Hence we have

$$\dot{C}_2(t) = -\left[\int_0^\infty d\omega_k \overline{g^2(\omega_k)}\mathcal{D}(\omega_k)\left(\pi\delta(\omega_k-\omega_0) - i\frac{P}{\omega_k-\omega_0}\right)\right]C_2(t). \tag{1.65}$$

We can write these as

$$\dot{C}_2(t) = \left(-i\delta - \frac{\Gamma}{2}\right)C_2(t), \tag{1.66}$$

where δ is the frequency shift in the atomic transition frequency arising from the coupling to the continuum. The eq. (1.66) has the solution

$$C_2(t) = e^{-\frac{\Gamma}{2}t}e^{-i\delta t}C_2(0). \tag{1.67}$$

The absolute square of the probability amplitude is

$$|C_2(t)|^2 = e^{-\Gamma t}|C_2(t)|^2, \tag{1.68}$$

where $\Gamma = 2\pi\overline{g^2(\omega_k)}\mathcal{D}(\omega_k)$ is the decay rate. From this equation it is seen that the upper level population decays exponentially with the rate Γ. In other words, the atom spontaneously and irreversible emits radiation in to the continuum.

1.4. The Damped Two-Level Atom

In this section, we discuss the behaviour of a two-level atom with coupling to a bath of harmonic oscillators (Foerster (1972)). In the case that the oscillators represent the electromagnetic field modes, we notice that the damping mechanism represents the spontaneous emission. Due to the coupling to the bath of harmonic oscillators, initially pure atomic state rapidly becomes mixed. There exist so many works that treat this problem in the density operator approach due to the coupling to the bath. We treat this problem in the Heisenberg picture since it provides to obtain equations of motion for the atomic

operators which are describing the dynamics of the atom (Barnett and Radmore (1997)). The corresponding Hamiltonian describing a two-level atom coupled to the quantized electromagnetic modes is

$$\hat{H} = \sum_k \hbar\omega_k \hat{a}_k^\dagger(t)\hat{a}_k(t) + \frac{1}{2}\hbar\omega_0\hat{\sigma}_3(t) + \hbar\sum_k g_k[\hat{\sigma}_+(t)\hat{a}_k(t) + \hat{a}_k^\dagger(t)\hat{\sigma}_-(t)]. \quad (1.69)$$

and the equal-time commutation relation for the field operators is $\left[\hat{a}(t), \hat{a}^\dagger(t)\right] = 1$. The Hamiltanian written above is expressed in symmetric order so that the effects of the vacuum field as well as the radiated field on the dynamics are included. From this Hamiltonian we derive the interaction picture Hamiltanian. By imposing the unitary operator

$$\hat{U} = exp\left\{\frac{i}{\hbar}\left(\frac{1}{2}\hbar\omega_0\hat{\sigma}_3 + \sum_k \hbar\omega_0\hat{a}_k^\dagger\hat{a}_k\right)t\right\}, \quad (1.70)$$

we end up with the following interaction picture Hamiltonian

$$\hat{\mathcal{V}} = \sum_k \hbar\Delta_k\hat{a}_k^\dagger(t)\hat{a}_k(t) + \hbar\sum_k g_k[\hat{\sigma}_+(t)\hat{a}_k(t) + \hat{a}_k^\dagger(t)\hat{\sigma}_-(t)], \quad (1.71)$$

where $\Delta_k = \omega_k - \omega_0$. Then, by using the Heisenberg equation of motion, we obtain the equations of motion for the atom and the field operators:

$$\dot{\hat{\sigma}}_- = \frac{i}{\hbar}[\mathcal{V}, \hat{\sigma}_-] = i\sum_k g_k\hat{\sigma}_3(t)\hat{a}_k(t), \quad (1.72)$$

$$\dot{\hat{\sigma}}_+ = \frac{i}{\hbar}[\mathcal{V}, \hat{\sigma}_+] = -i\sum_k g_k\hat{a}_k^\dagger(t)\hat{\sigma}_3(t), \quad (1.73)$$

$$\dot{\hat{\sigma}}_3 = -2i\sum_k g_k[\hat{\sigma}_+(t)\hat{a}_k(t) - \hat{a}_k^\dagger(t)\hat{\sigma}_-(t)], \quad (1.74)$$

$$\dot{\hat{a}}_k = -i\Delta_k\hat{a}_k(t) - ig_k\hat{\sigma}_-(t), \quad (1.75)$$

$$\dot{\hat{a}}_k^\dagger = i\Delta_k\hat{a}_k^\dagger(t) + ig_k\hat{\sigma}_+(t). \quad (1.76)$$

The excitations in the bath arising from its interaction with the atom are assumed

to be so small so that the state of the bath may be approximated by its initial state (Mollow and Miller (1969)). In order to describe the atomic dynamics, we need to obtain the expectation values of the atomic operators. Thus, we start by formally integrating the eqs. (1.75) and (1.76). We have:

$$\hat{a}_k(t) = e^{-i\Delta_k t}\hat{a}_k(0) - ig_k \int_0^t e^{-i\Delta_k(t-t')}\sigma_-(t')dt', \tag{1.77}$$

$$\hat{a}_k^\dagger(t) = e^{i\Delta_k t}\hat{a}_k^\dagger(0) + ig_k \int_0^t e^{i\Delta_k(t-t')}\sigma_+(t')dt'. \tag{1.78}$$

Now we wiil put the eqs. (1.77) and (1.78) into eqs. (1.72), (1.73), and (1.74) that will yield the following expressions for the atomic operators:

$$\begin{aligned}\dot{\hat{\sigma}}_-(t) &= i\sum_k g_k e^{-i\Delta_k t}\hat{\sigma}_3(t)\hat{a}_k(0) \\ &\quad + \sum_k g_k^2 \int_0^t e^{-i\Delta_k(t-t')}\hat{\sigma}_3(t)\hat{\sigma}_-(t')dt', \end{aligned}\tag{1.79}$$

$$\begin{aligned}\dot{\hat{\sigma}}_+(t) &= -i\sum_k g_k e^{i\Delta_k t}\hat{a}_k^\dagger(0)\hat{\sigma}_3(t) \\ &\quad + \sum_k g_k^2 \int_0^t e^{i\Delta_k(t-t')}\hat{\sigma}_+(t')\hat{\sigma}_3(t)dt', \end{aligned}\tag{1.80}$$

$$\begin{aligned}\dot{\hat{\sigma}}_3(t) &= -2i\sum_k \{[g_k e^{-i\Delta_k t}\hat{\sigma}_+(t)\hat{a}_k(0) \\ &\quad - ig_k^2 \int_0^t e^{-i\Delta_k(t-t')}\hat{\sigma}_+(t)\hat{\sigma}_-(t')] + h.c.\}. \end{aligned}\tag{1.81}$$

The first terms in each above equation can be expressed in terms of the Langevin operator

$$\hat{F}(t) = -i\sum_k g_k e^{-i\Delta_k t}\hat{a}_k(0), \tag{1.82}$$

and its Hermitian conjugate

$$\hat{F}^\dagger(t) = i\sum_k g_k e^{i\Delta_k t}\hat{a}_k^\dagger(0). \tag{1.83}$$

Then the Eqs. (1.79) to (1.81) becomes

$$\dot{\hat{\sigma}}_-(t) = -\hat{\sigma}_3(t)\hat{F}(t) + \sum_k g_k^2 \int_0^t e^{-i\Delta_k(t-t')}\hat{\sigma}_3(t)\hat{\sigma}_-(t')dt', \tag{1.84}$$

$$\dot{\hat{\sigma}}_+(t) = -\hat{F}^\dagger(t)\hat{\sigma}_3(t) + \sum_k g_k^2 \int_0^t e^{i\Delta_k(t-t')}\hat{\sigma}_+(t')\hat{\sigma}_3(t)dt', \tag{1.85}$$

$$\begin{aligned}\dot{\hat{\sigma}}_3(t) &= 2\hat{\sigma}_+(t)\hat{F}(t) + 2\hat{F}^\dagger(t)\hat{\sigma}_-(t) \\ &\quad - 2\sum_k g_k^2 \left[\int_0^t e^{-i\Delta_k(t-t')}\hat{\sigma}_3(t)\hat{\sigma}_-(t')dt' + h.c.\right].\end{aligned} \tag{1.86}$$

Now, in the continuum limit, the above equations become

$$\begin{aligned}\dot{\hat{\sigma}}_-(t) &= -\hat{\sigma}_3(t)\hat{F}(t) \\ &\quad + \int_0^\infty g^2(\omega_k)\mathcal{D}(\omega_k)d\omega_k \int_0^t e^{-i\Delta_k(t-t')}\hat{\sigma}_3(t)\hat{\sigma}_-(t')dt',\end{aligned} \tag{1.87}$$

$$\begin{aligned}\dot{\hat{\sigma}}_+(t) &= -\hat{F}^\dagger(t)\hat{\sigma}_3(t) \\ &\quad + \int_0^\infty g^2(\omega_k)\mathcal{D}(\omega_k)d\omega_k \int_0^t e^{i\Delta_k(t-t')}\hat{\sigma}_+(t')\hat{\sigma}_3(t)dt',\end{aligned} \tag{1.88}$$

$$\begin{aligned}\dot{\hat{\sigma}}_3(t) &= 2\hat{\sigma}_+(t)\hat{F}(t) + 2\hat{F}^\dagger(t)\hat{\sigma}_-(t) \\ &\quad - 2\int_0^\infty g^2(\omega_k)\mathcal{D}(\omega_k)d\omega_k \left[\int_0^t e^{-i\Delta_k(t-t')}\hat{\sigma}_3(t)\hat{\sigma}_-(t')dt' + h.c.\right].\end{aligned} \tag{1.89}$$

Up to now our calculation has been exact, other than the dipole and the rotating wave approximations. From now on we make the Born-Markov approximation, and we derive the equations of motion in a more compact form.

We start by rewriting the equations (1.87) to (1.89) as following

$$\dot{\hat{\sigma}}_-(t) = -\hat{\sigma}_3(t)\hat{F}(t) + \int_0^t dt' K(t-t')\hat{\sigma}_3(t)\hat{\sigma}_-(t'), \tag{1.90}$$

$$\dot{\hat{\sigma}}_+(t) = -\hat{F}^\dagger(t)\hat{\sigma}_3(t) + \int_0^t dt' K^*(t-t')\hat{\sigma}_+(t')\hat{\sigma}_3(t), \tag{1.91}$$

$$\begin{aligned}\dot{\hat{\sigma}}_3(t) &= 2\hat{\sigma}_+(t)\hat{F}(t) + 2\hat{F}^\dagger(t)\hat{\sigma}_-(t) \\ &\quad - 2\left[\int_0^t dt' K(t-t')\hat{\sigma}_+(t)\hat{\sigma}_-(t') + h.c.\right],\end{aligned} \tag{1.92}$$

where the kernel $K(t-t')$ is given by

$$K(t-t') = \int_0^\infty d\omega_k g^2(\omega_k)\mathcal{D}(\omega_k)e^{-i(\omega_k-\omega_0)(t-t')}, \tag{1.93}$$

and it is the Fourier transform of the ω_k-dependent coupling constant, weighted by the density of states. For example, the value of $\dot{\hat{\sigma}}_-$ depends on the values of $\hat{\sigma}_-$ at all earlier times. However, if the kernel is sharply peaked at $t' = t$ then only values of t' close to t contributes to the integral in (1.90). Because the density of states is very broad, and the coupling varies slowly, the kernel will be sharply peaked at $t = t'$. In other words, the atom-field correlation time is very small. That is to say atom-vacuum correlations lose memory. This is the Markov approximation. In the Markov approximation, we replace the value of $\hat{\sigma}_-(t')$ by its value at $t' = t$. Thus, the integral in (1.90) becomes

$$\int_0^t dt' K(t-t')\hat{\sigma}_3(t)\hat{\sigma}_-(t') = \hat{\sigma}_3(t)\hat{\sigma}_-(t)\int_0^t dt' K(t-t') = \hat{\sigma}_-(t)\int_0^t d\tau K(\tau). \tag{1.94}$$

In the Markov approximation, the kernel $K(\tau)$ is a sharply peaked function at $\tau = 0$. Thus, the integral in (1.94) must be independent of its upper limit $\tau = t$. For the evaluation of the integral, the upper limit should be allowed to tend to infinity. In order to satisfy the convergence of the integral, the convergence factor is inserted $exp(-\epsilon\tau)$. After the integration has been performed, we let the $\epsilon \to 0^+$. The integral in (1.94) becomes

$$\lim_{\epsilon \to\ 0^+} \int_0^\infty \left(\int g_k^2(\omega_k)\mathcal{D}(\omega_k)e^{-i(\omega_k-\omega_0)(t-t')}d\omega_k \right) d\tau$$

$$= \lim_{\epsilon \to\ 0^+} -i \int \frac{g_k^2(\omega_k)\mathcal{D}(\omega_k)}{(\omega_k - \omega_0) - i\epsilon} d\omega_k$$

$$= \pi g_k^2(\omega_0)\mathcal{D}(\omega_0) - iP \int \frac{g_k^2(\omega_k)\mathcal{D}(\omega_k)}{(\omega_k - \omega_0)} d\omega_k = \Gamma + i\delta\omega. \tag{1.95}$$

The coupling to the quantum electromagnetic vacuum gives rise to a term $-\Gamma\hat{\sigma}_-(t)$ and a shift in the frequency of atomic transition by $\delta\omega$. For convenience we set this frequency shift to zero, and practically, this can be realized by moving to an interaction picture in which the zero of energy is chosen to be the shifted energy.

Now consider the eq. (1.90). After making the Born-Markov approximation, it becomes

$$\dot{\hat{\sigma}}_-(t) = -\Gamma\hat{\sigma}_-(t) - \hat{\sigma}_3(t)\hat{F}(t). \tag{1.96}$$

The same goes for the eqs. (1.91) and (1.92), after the Markov approximation they become

$$\dot{\hat{\sigma}}_+(t) = -\Gamma\hat{\sigma}_+(t) - \hat{F}^\dagger(t)\hat{\sigma}_3(t) \tag{1.97}$$

$$\dot{\hat{\sigma}}_3(t) = -2\Gamma\left[\hat{\sigma}_3(t) + 1\right] + 2\hat{F}^\dagger(t)\hat{\sigma}_-(t) + 2\hat{\sigma}_+(t)\hat{F}(t) \tag{1.98}$$

Each of the equations in (1.96) to (1.98) consists of a damping term and a Langevin term which is a multiplication of the Langevin operator (or the Hermitian conjugate of the Langevin operator) by the atomic operators. The expectation values of the atomic operators give the properties of the atom at any given time. Therefore, its sufficient to obtain the equations of motion for the expectation values of the atomic operators. However, due to the multiplication of the Langevin operator by the atomic operators, the solution of the equations of the motion is not possible because the atomic operators themselves depends on the Langevin operator. That is, we do not know how to deal with the expectation value of this product. The decorrelation of the product, for example, can be made, that is $\langle\hat{\sigma}_3(t)\hat{F}(t)\rangle \simeq \langle\hat{\sigma}_3(t)\rangle\langle\hat{F}(t\rangle$. However, if the field is at finite temperature, the decorre-

lation of the product will result to neglect the part of the influence of the field. In order to solve this problem, we proceed by first formally integrating eqs. (1.96), (1.97), and (1.98). This gives

$$\hat{\sigma}_-(t) = e^{-\Gamma t}\hat{\sigma}_-(0) - \int_0^t e^{-\Gamma(t-t')}\hat{\sigma}_3(t')\hat{F}(t')dt' \tag{1.99}$$

$$\hat{\sigma}_+(t) = e^{-\Gamma t}\hat{\sigma}_+(0) - \int_0^t e^{-\Gamma(t-t')}\hat{F}^\dagger(t')\hat{\sigma}_3(t')dt' \tag{1.100}$$

$$\begin{aligned}\hat{\sigma}_3(t) + 1 &= e^{-2\Gamma t} \\ &\times \left(\hat{\sigma}_3(0) + 1 + 2\int_0^t e^{2\Gamma t'}\left[\hat{\sigma}_+(t')\hat{F}(t') + \hat{F}^\dagger(t')\hat{\sigma}_-(t')\right]dt'\right),\end{aligned} \tag{1.101}$$

and we continue by substituting these into (1.96) to (1.98) and then taking the expectation value of each equation gives

$$\begin{aligned}\langle\dot{\hat{\sigma}}_-(t)\rangle &= -\Gamma\langle\hat{\sigma}_-(t)\rangle - 2\int_0^t e^{-2\Gamma(t-t')} \\ &\times \left[\langle\hat{\sigma}_+(t')\hat{F}(t')\hat{F}(t)\rangle + \langle\hat{F}^\dagger(t')\hat{F}(t)\hat{\sigma}_-(t')\rangle\right]dt',\end{aligned} \tag{1.102}$$

$$\begin{aligned}\langle\dot{\hat{\sigma}}_+(t)\rangle &= -\Gamma\langle\hat{\sigma}_+(t)\rangle - 2\int_0^t e^{-2\Gamma(t-t')} \\ &\times \left[\langle\hat{F}^\dagger(t)\hat{F}^\dagger(t')\hat{\sigma}_-(t')\rangle + \langle\hat{\sigma}_+(t')\hat{F}^\dagger(t)\hat{F}(t')\rangle\right]dt',\end{aligned} \tag{1.103}$$

$$\begin{aligned}\langle\dot{\hat{\sigma}}_3(t)\rangle &= -2\Gamma\left[\langle\hat{\sigma}_3(t)\rangle + 1\right] - 2\int_0^t e^{-\Gamma(t-t')} \\ &\times \left[\langle\hat{F}^\dagger(t')\hat{\sigma}_3(t')\hat{F}(t)\rangle + \langle\hat{F}^\dagger(t)\hat{\sigma}_3(t')\hat{F}(t')\rangle\right]dt'.\end{aligned} \tag{1.104}$$

We can continue to repeat the above two steps which are formal integration and back-substitution, and this leads to equations containing higher-order correlation functions. The correlations functions represent the influence of the field, as modified by the atom, in turn modifying the atomic dynamics. Since the influence of the atom on the field is small, the higher-order corrections can be neglected by making the decorrelation of the correlation functions at this stage. That is, we can approximate, for example, $\langle\hat{\sigma}_+(t')\hat{F}(t')\hat{F}(t)\rangle$ by $\langle\hat{\sigma}_+(t')\rangle\langle\hat{F}(t')\hat{F}(t)\rangle$, and similar expressions for the other correla-

tions functions. With this approximation, the equations of motion become

$$\langle\dot{\hat{\sigma}}_-(t)\rangle = -\Gamma\langle\hat{\sigma}_-(t)\rangle - 2\int_0^t e^{-2\Gamma(t-t')} \times \left[\langle\hat{\sigma}_+(t')\rangle\langle\hat{F}(t')\hat{F}(t)\rangle + \langle\hat{F}^\dagger(t')\hat{F}(t)\rangle\langle\hat{\sigma}_-(t')\rangle\right] dt', \tag{1.105}$$

$$\langle\dot{\hat{\sigma}}_+(t)\rangle = -\Gamma\langle\hat{\sigma}_+(t)\rangle - 2\int_0^t e^{-2\Gamma(t-t')} \times \left[\langle\hat{F}^\dagger(t)\hat{F}^\dagger(t')\rangle\langle\hat{\sigma}_-(t')\rangle + \langle\hat{\sigma}_+(t')\rangle\langle\hat{F}^\dagger(t)\hat{F}(t')\rangle\right] dt', \tag{1.106}$$

$$\langle\dot{\hat{\sigma}}_3(t)\rangle = -2\Gamma\left[\langle\hat{\sigma}_3(t)\rangle + 1\right] - 2\int_0^t e^{-\Gamma(t-t')} \times \left[\langle\hat{F}^\dagger(t')\hat{F}(t)\rangle + \langle\hat{F}^\dagger(t)\hat{F}(t')\rangle\right]\langle\hat{\sigma}_3(t')\rangle dt'. \tag{1.107}$$

As it can be seen from the above equations, the influence of the field is given by the correlation functions for the Langevin operators which are determined by the initial state of the field.

For a thermal field, the correlation functions can be determined by using the following expectation values for the initial field operators at thermodynamic equilibrium:

$$\langle\hat{a}_k(0)\rangle = \langle\hat{a}_k^\dagger(0)\rangle = 0 \tag{1.108}$$

$$\langle\hat{a}_k(0)\hat{a}_{k'}(0)\rangle = \langle\hat{a}_k^\dagger(0)\hat{a}_{k'}^\dagger(0)\rangle = 0 \tag{1.109}$$

$$\langle\hat{a}_k^\dagger(0)\hat{a}_{k'}(0)\rangle = \bar{n}_k\delta_{kk'} \tag{1.110}$$

$$\langle\hat{a}_k(0)\hat{a}_{k'}^\dagger(0)\rangle = (\bar{n}_k + 1)\delta_{kk'}. \tag{1.111}$$

Then the lowest order non-zero correlation functions are

$$\langle\hat{F}^\dagger(t')\hat{F}(t)\rangle = \int g^2(\omega_k)\mathcal{D}(\omega_k)\bar{n}(\omega_k)e^{-i(\omega_k-\omega_0)(t-t')}d\omega_k \tag{1.112}$$

$$\langle\hat{F}(t)\hat{F}^\dagger(t')\rangle = \int g^2(\omega_k)\mathcal{D}(\omega_k)\left[\bar{n}(\omega_k) + 1\right]e^{-i(\omega_k-\omega_0)(t-t')}d\omega_k. \tag{1.113}$$

By substituting the eq. (1.112) into (1.105) to (1.107) and once more making the

Markov approximation, we have

$$\langle \dot{\hat{\sigma}}_-(t)\rangle = -\Gamma\left[2\bar{n}(0)+1\right]\langle \hat{\sigma}_-(t)\rangle \tag{1.114}$$

$$\langle \dot{\hat{\sigma}}_+(t)\rangle = -\Gamma\left[2\bar{n}(0)+1\right]\langle \hat{\sigma}_+(t)\rangle \tag{1.115}$$

$$\langle \dot{\hat{\sigma}}_3(t)\rangle = -2\Gamma\left\{\left[2\bar{n}(0)+1\right]\langle \hat{\sigma}_3(t)\rangle\right] + 1\}. \tag{1.116}$$

From the above equations, it is clear that the rate of decay of the atomic dipole is enhanced by a factor $2\bar{n}(0)+1$, where $\bar{n}(0)$ is the mean occupation number of a field mode with frequency equal to the shifted atomic transition frequency. At the state state it can be seen from the solution of the equations that the atomic dipole moment is zero, that is $\langle \hat{\sigma}_-(\infty)\rangle = \langle \hat{\sigma}_+(\infty)\rangle = 0$ and inversion $\langle \hat{\sigma}_3(\infty)\rangle = -\left[2\bar{n}(0)+1\right]^{-1}$.

1.5. Power Spectrum of Emitted Light

In this section, we relate the power spectrum of the emitted light by the atom with the atomic two-time correlation function.

We start by writing the field annihilation operator $\hat{a}_k$ which is obtained by formally integrating the corresponding Heisenberg equation of motion, that is,

$$\hat{a}_k(t) = e^{-i\omega_k t}\hat{a}_k(0) - ig_k\int_0^t e^{-i\omega_k(t-t')}\sigma_-(t')dt'. \tag{1.117}$$

We interpret the first term as the contribution from the vacuum fluctuations. Even in the absence of the atom, this term is present. On the other hand, the second term represents the contribution coming from the atom, in other words the self-field of the radiating atom. However, the Heisenberg field operator may be found by substituting the above annihilation operator into the electric field operator (Mollow (1969)). The positive frequency component of the electric field operator is

$$\hat{\mathbf{E}}^+(\mathbf{r},t) = \sum_k \left(\frac{\hbar\omega_k}{2\epsilon_0 V}\right)^{1/2}\mathbf{e}_k\hat{a}_k(t)e^{ikr}, \tag{1.118}$$

and by substituting $\hat{a}_k(t)$ given in eq. (1.117), we obtain

$$\hat{\mathbf{E}}^{+}_{vac}(\mathbf{r},t) = \sum_k \left(\frac{\hbar\omega_k}{2\epsilon_0 V}\right)^{1/2} \mathbf{e}_k \hat{a}_k e^{i(kr-\omega t)} \tag{1.119}$$

$$\hat{\mathbf{E}}^{+}_{s}(\mathbf{r},t) = \frac{\omega_0^2}{c^2 r}\left((\mathbf{e}_k \times \mathbf{d}) \times \mathbf{e}_k\right)\hat{\sigma}_-(t-\frac{r}{c}). \tag{1.120}$$

The summation of these two terms gives the total field. By the assumption that the field is unexcited initially, for both of the vacuum and the thermal fields, the contribution coming from the eq. (1.119) goes to zero. Thus, we only consider the source field which is given by (1.120). The spectral intensity of the emitted light per unit solid angle is given by

$$\frac{dI(\omega)}{d\Omega} = \frac{cr^2}{8\pi^2}\int_{-\infty}^{\infty} d\tau e^{i\omega\tau}\langle \hat{\mathbf{E}}^{+}(\mathbf{r},t)\hat{\mathbf{E}}^{-}(\mathbf{r},t+\tau)\rangle_s. \tag{1.121}$$

By substituting eq. (1.120) into the eq. (1.121), one can find

$$\frac{dI(\omega)}{d\Omega} = \frac{\omega_0^4}{8\pi^2 c^3}|\left(\mathbf{e}_k \times \mathbf{d}\right) \times \mathbf{e}_k|^2 S(\omega), \tag{1.122}$$

where

$$S(\omega) = \int_{-\infty}^{\infty} d\tau e^{-i\omega\tau}\langle \hat{\sigma}_+(\tau+t)\hat{\sigma}_-(t)\rangle_s. \tag{1.123}$$

In obtaning the eq. (1.123), it is assumed that the correlation function depends only on τ in steady state.

The correlation function in eq. (1.123) can be obtained by using the quantum regression theorem which the two time expectation values to expectations evaluated at a single time (Breuer and Petruccione (1985)). We can write the equation of motion for the

two-time correlation function by using the eq. (1.96) which gives

$$\frac{d}{d\tau}\langle\hat{\sigma}_+(t+\tau)\hat{\sigma}_-(t)\rangle = -\Gamma\langle\hat{\sigma}_+(t+\tau)\hat{\sigma}_-(t)\rangle - \langle\hat{F}^\dagger(t+\tau)\hat{\sigma}_3(t+\tau)\hat{\sigma}_-(t)\rangle. \tag{1.124}$$

From the eq. (1.101), we insert the expression for $\hat{\sigma}_3(t+\tau)$ into the last term of the eq. (1.124) and then we obtain

$$\langle\hat{F}^\dagger(t+\tau)\hat{\sigma}_3(t+\tau)\hat{\sigma}_-(t)\rangle = 2\langle\hat{F}^\dagger(t+\tau)\left(\int_0^{t+\tau} e^{[-2\Gamma(t+\tau-t')]} \times\left[\hat{\sigma}_+(t')\hat{F}(t') + \hat{F}^\dagger(t')\hat{\sigma}_-(t')\right]dt'\right)\hat{\sigma}_-(t)\rangle. \tag{1.125}$$

In obtaining the eq. (1.125), the fact that $\hat{\sigma}_-(t)$ depends on the Langevin operator for times prior to t has been employed. That is,

$$\langle\hat{F}^\dagger(t+\tau)\hat{\sigma}_3(0)\hat{\sigma}_-(t)\rangle = \langle\hat{F}^\dagger(t+\tau)\hat{\sigma}_-(t)\rangle = 0. \tag{1.126}$$

By making the Born-Markov approximation in (1.125), for a thermal field it becomes

$$\langle\hat{F}^\dagger(t+\tau)\hat{\sigma}_3(t+\tau)\hat{\sigma}_-(t)\rangle = 2\Gamma\bar{n}(0)\langle\hat{\sigma}_+(t+\tau)\hat{\sigma}_-(t)\rangle \tag{1.127}$$

Now, we substitute eq. (1.127) into eq. (1.124) which yields

$$\frac{d}{d\tau}\langle\hat{\sigma}_+(t+\tau)\hat{\sigma}_-(t)\rangle = -\Gamma\left[2\bar{n}(0)+1\right]\langle\hat{\sigma}_+(t+\tau)\hat{\sigma}_-(t)\rangle, \tag{1.128}$$

and by solving this equation, we have

$$\langle\hat{\sigma}_+(t+\tau)\hat{\sigma}_-(t)\rangle = e^{-\Gamma[2\bar{n}(0)+1]\tau}\langle\hat{\sigma}_+(t)\hat{\sigma}_-(t)\rangle. \tag{1.129}$$

The steady state value of $\langle\hat{\sigma}_+(t)\hat{\sigma}_-(t)\rangle$ is $\bar{n}(0)/(2\bar{n}(0)+1)$. We put the steady

state value of it into eq. (1.129), which gives

$$\langle \hat{\sigma}_+(t+\tau)\hat{\sigma}_-(t)\rangle = e^{-\Gamma[2\bar{n}(0)+1]\tau}\frac{\bar{n}(0)}{2\bar{n}(0)+1}. \tag{1.130}$$

By putting eq. (1.130) into eq. (1.123), we obtain the following expression

$$S(\omega) = \frac{2\bar{n}(0)}{2\bar{n}(0)+1} Re \frac{1}{i\omega + \Gamma\left[2\bar{n}(0)+1\right]}. \tag{1.131}$$

The normalized spectrum is

$$S(\omega) = \frac{\left[2\bar{n}(0)+1\right]\Gamma/\pi}{\Omega^2 + \Gamma^2\left[2\bar{n}(0)+1\right]^2}. \tag{1.132}$$

In Fig. 1.1, we plot the normalized spectrum of the light emitted by the atom interacting with the surrounding broad-band field. The spectrum corresponds to the spontaneous emission from a two-level atom. It is a Lorentzian centered at the atomic transition and has a width which depends on the temperature of the surronding field.

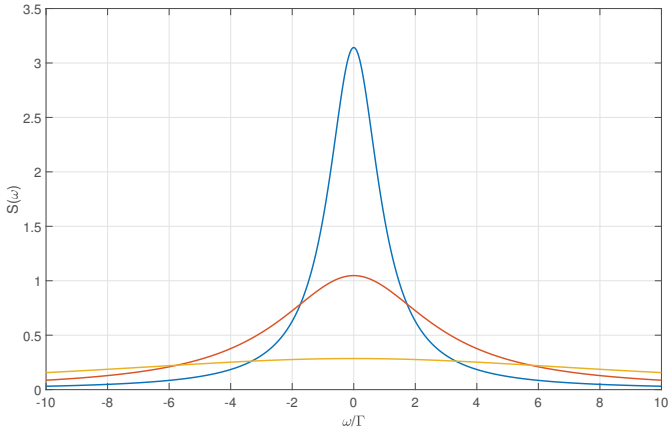

Figure 1.1. Spectrum of the emitted light by an atom interacting with broad-band thermal field with $\bar{n}(0) = 0$ (blue curve), $\bar{n}(0) = 1$ (red curve), and $\bar{n}(0) = 5$ (orange curve).

CHAPTER 2

SPONTANEOUS EMISSION FROM A THREE-LEVEL ATOM

2.1. Theory

Consider a three-level atom with two upper levels. In the Dirac notation, the upper levels are labelled by $|3\rangle$ and $|2\rangle$, and the lower level is by $|1\rangle$. The level $|3\rangle$ has higher energy than $|2\rangle$.

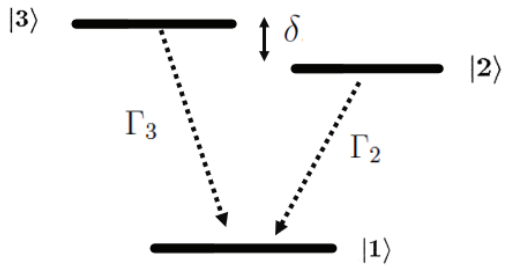

Figure 2.1. Representative scheme of the atomic model considered in this chapter. It represents a three-level atom in V-type configuration in which the two upper levels are coupled by the same vacuum modes to the lower level, respectively. The energy of the level $|3\rangle$ is higher than the energy of the level $|2\rangle$ by $\hbar\delta$.

The same vacuum modes couples the two upper levels to the lower level. In the dipole and the rotating-wave approximations, the Schrödinger picture Hamiltonian describing the atom-field system consists of the two terms. The first one corresponds to the free-evolution of the atom and the field in the absence of interaction. The second term is

called as the interaction Hamiltonian, and comes into play in the presence of interaction. That is,

$$H = H_0 + H_I, \tag{2.1}$$

and each term is given by the following expressions

$$H_0 = \hbar\omega_{21}|2\rangle\langle 2| + \hbar\omega_{31}|3\rangle\langle 3| + \sum_k \hbar\omega_k \hat{a}_k^\dagger \hat{a}_k \tag{2.2}$$

$$\begin{aligned} H_I = {} & \hbar \sum_k g_{k,2} \left[\hat{a}_k |2\rangle\langle 1| + \hat{a}_k^\dagger |1\rangle\langle 2|\right] \\ & + \hbar \sum_k g_{k,3} \left[\hat{a}_k |3\rangle\langle 1| + \hat{a}_k^\dagger |1\rangle\langle 3|\right] \end{aligned} \tag{2.3}$$

where H_0 contains the free-atom and the free-field Hamiltonians.From the free-field Hamiltonian zero-point energy term has been omitted since it does not contribute to the dynamics of the system. The term H_I is the energy of the interaction between the atom and the modes of the universe in the vacuum state. For convenience we work in the interaction picture. The Schrödinger interaction picture Hamiltonian describing the system consists of the atom and the vacuum modes is

$$\begin{aligned} \mathcal{V} = {} & \hbar \sum_k g_k^{(2)} [\hat{\sigma}_{12} \hat{a}_k e^{i(\omega_{21} - \omega_k)t} + \hat{\sigma}_{21} \hat{a}_k^\dagger e^{-i(\omega_{21} - \omega_k)t}] \\ & + \hbar \sum_k g_k^{(3)} [\hat{\sigma}_{13} \hat{a}_k e^{i(\omega_{31} - \omega_k)t} + \hat{\sigma}_{31} \hat{a}_k^\dagger e^{-i(\omega_{31} - \omega_k)t}], \end{aligned} \tag{2.4}$$

where the frequency difference between the states $|2\rangle$, $|3\rangle$ and $|1\rangle$ are ω_{21} and ω_{31}, respectively. The creation (annihilation) operators for the k^{th} vacuum mode of frequency ω_k is $\hat{a}_k^\dagger$ ($\hat{a}_k$), and k stands both for the polarization and the momentum of the modes of the vacuum. Here, $g_k^{(2,3)}$ are the coupling constants between the k^{th} mode of the vacuum and the atomic transitions from the states $|3\rangle$ and $|2\rangle$ to $|1\rangle$, and they are assumed to be real. The interaction Hamiltonian is responsible for the spontaneous emission of the atom initially in the upper levels. The initial state of the atom-field system can be written as

$$|\psi(0)\rangle = \alpha(0)|2\rangle|0\rangle + \beta(0)|3\rangle|0\rangle. \tag{2.5}$$

The time evolution of the state vector is given by the Schrödinger equation

$$i\hbar\frac{d}{dt}|\psi(t)\rangle = \mathcal{V}|\psi(t)\rangle. \tag{2.6}$$

The state vector at time t is

$$|\psi(t)\rangle = \alpha(t)|2\rangle|0\rangle + \beta(t)|3\rangle|0\rangle + \sum_k \gamma_k(t)\hat{a}_k^\dagger|0\rangle|1\rangle. \tag{2.7}$$

By substituting the Eqs. (2.7) and (2.4) into Eq. (2.6), we can obtain

$$\frac{d}{dt}\alpha(t) = -i\sum_k g_k^{(2)}\gamma_k(t)e^{i(\omega_{21}-\omega_k)t} \tag{2.8}$$

$$\frac{d}{dt}\beta(t) = -i\sum_k g_k^{(3)}\gamma_k(t)e^{i(\omega_{31}-\omega_k)t} \tag{2.9}$$

$$\frac{d}{dt}\gamma_k(t) = -ig_k^{(2)}\alpha(t)e^{-i(\omega_{21}-\omega_k)t} - ig_k^{(3)}\beta(t)e^{-i(\omega_{31}-\omega_k)t}. \tag{2.10}$$

By formally integrating Eq.(2.10), we obtain

$$\begin{aligned}\gamma_k(t) = &-ig_k^{(2)}\int_0^t \alpha(t')e^{-i(\omega_{21}-\omega_k)t'}dt' \\ &- ig_k^{(3)}\int_0^t \beta(t')e^{-i(\omega_{31}-\omega_k)t'}dt'.\end{aligned} \tag{2.11}$$

Substituting Eq. (2.11) into Eqs. (2.8) and (2.9), we have

$$\begin{aligned}\frac{d}{dt}\alpha(t) = &-\sum_k g_{k2}^2\int_0^t \alpha(t')e^{i(\omega_{21}-\omega_k)(t-t')}dt' \\ &-\sum_k g_{k2}g_{k3}\int_0^t \beta(t')e^{-i(\omega_{31}-\omega_k)t}e^{i(\omega_{21}-\omega_k)t}dt'\end{aligned} \tag{2.12}$$

$$\begin{aligned}\frac{d}{dt}\beta(t) = &-\sum_k g_{k3}^2\int_0^t \beta(t')e^{i(\omega_{31}-\omega_k)(t-t')}dt' \\ &-\sum_k g_{k2}g_{k3}\int_0^t \alpha(t')e^{-i(\omega_{21}-\omega_k)t'}e^{i(\omega_{31}-\omega_k)t}dt'.\end{aligned} \tag{2.13}$$

By making the Born-Markov approximation in the continuum limit, we obtain

$$\frac{d}{dt}\alpha(t) = -\frac{\Gamma_2}{2}\alpha(t) - p\frac{\sqrt{\Gamma_2\Gamma_3}}{2}\beta(t)e^{i\delta t} \tag{2.14}$$

$$\frac{d}{dt}\beta(t) = -\frac{\Gamma_3}{2}\beta(t) - p\frac{\sqrt{\Gamma_2\Gamma_3}}{2}\alpha(t)e^{-i\delta t} \tag{2.15}$$

$$p = \frac{\mathbf{d}_{21}.\mathbf{d}_{31}}{|\mathbf{d}_{21}||\mathbf{d}_{31}|} = cos(\theta) \tag{2.16}$$

$$\Gamma_2 = 2\pi\left[g_k^{(2)}(\omega_{21})\right]^2 D(\omega_{21}) \tag{2.17}$$

$$\Gamma_3 = 2\pi\left[g_k^{(3)}(\omega_{31})\right]^2 D(\omega_{31}) \tag{2.18}$$

$$\delta_k = \omega_k - \frac{1}{2}\left(\omega_3 + \omega_2\right) \tag{2.19}$$

where δ is the difference between the frequencies of the upper levels. In obtaining the eqs. (2.14) and (2.15), it has been assumed that the δ is much more smaller than the frequencies of the upper levels ω_{21} and ω_{31}, that is $\delta << \omega_{21}, \omega_{31}$. Also, we have assumed that the dipole moments of the two transitions are parallel to each other.

By making the transformations

$$\alpha(t) = \tilde{\alpha}(t)e^{i\delta/2t} \tag{2.20}$$

$$\beta(t) = \tilde{\beta}(t)e^{-i\delta/2t}, \tag{2.21}$$

the eqs. (2.14) and (2.15) becomes

$$\frac{d}{dt}\tilde{\alpha}(t) = -\left(\frac{\Gamma_2}{2} + i\frac{\delta}{2}\right)\tilde{\alpha}(t) - \frac{\sqrt{\Gamma_2\Gamma_3}}{2}\tilde{\beta}(t) \tag{2.22}$$

$$\frac{d}{dt}\tilde{\beta}(t) = -\left(\frac{\Gamma_3}{2} - i\frac{\delta}{2}\right)\tilde{\beta}(t) - \frac{\sqrt{\Gamma_2\Gamma_3}}{2}\tilde{\alpha}(t). \tag{2.23}$$

We write this system of coupled linear differential equations in the equivalent vector-matrix form as

$$\frac{d}{dt}\begin{bmatrix}\tilde{\alpha}(t)\\ \tilde{\beta}(t)\end{bmatrix} = \begin{bmatrix}-A & -\Gamma\\ -\Gamma & -B\end{bmatrix}\begin{bmatrix}\tilde{\alpha}(t)\\ \tilde{\beta}(t)\end{bmatrix}, \tag{2.24}$$

where

$$A = \frac{\Gamma_2}{2} + i\frac{\delta}{2} \tag{2.25}$$

$$B = \frac{\Gamma_3}{2} - i\frac{\delta}{2} \tag{2.26}$$

$$\Gamma = \frac{\sqrt{\Gamma_2\Gamma_3}}{2}. \tag{2.27}$$

We propose an exponential solution in the vector-matrix form to the system of differential equations in (2.20). Therefore, our ansatz is

$$v(t) = ve^{\lambda' t} = \begin{bmatrix} v_1 \\ v_2 \end{bmatrix} e^{\lambda' t}. \tag{2.28}$$

By putting this equation into (2.20), we obtain the following eigenvalue equation

$$(D - \lambda' I)v = 0. \tag{2.29}$$

The eigenvalues are

$$\lambda_{1,2} = \frac{-(A+B) \pm \sqrt{(A+B)^2 - 4(AB - \Gamma^2)}}{2}, \tag{2.30}$$

and we found the corresponding eigenvectors as

$$v_1 = \begin{bmatrix} 1 \\ \frac{-A-\lambda_1}{\Gamma} \end{bmatrix}, v_2 = \begin{bmatrix} 1 \\ \frac{-A-\lambda_2}{\Gamma} \end{bmatrix}. \tag{2.31}$$

Then, we obtain the solution for $\alpha(t)$ and $\beta(t)$ as

$$\alpha(t) = \left[C_1 e^{S_1 t} + C_2 e^{S_2 t}\right] e^{-\frac{\Gamma_2}{2}t} \tag{2.32}$$

$$\beta(t) = -\frac{2}{\sqrt{\Gamma_2 \Gamma_3}} \left[C_1 S_2 e^{S_1 t} + C_2 S_2 e^{S_2 t}\right] e^{-\left(i\delta + \frac{\Gamma_2}{2}\right)t} \tag{2.33}$$

where

$$C_1 = \frac{\alpha(0) S_2 + 0.5\sqrt{\Gamma_2 \Gamma_3}\beta(0)}{S_2 - S_1} \tag{2.34}$$

$$C_2 = \frac{\alpha(0) S_1 + 0.5\sqrt{\Gamma_2 \Gamma_3}\beta(0)}{S_1 - S_2} \tag{2.35}$$

$$S_{1,2} = \frac{1}{2}\left(\lambda \pm \sqrt{\lambda^2 + \Gamma_2 \Gamma_3}\right) \tag{2.36}$$

$$\lambda = \frac{1}{2}\left(\Gamma_2 - \Gamma_3\right) + i\delta. \tag{2.37}$$

2.2. Evolution of the Upper-Level Populations

In the previous section, we have derived probability amplitudes for the upper two states in a general form. From eqs. (2.28) and (2.29), the populations of the upper levels can be obtained which are given by $|\alpha(t)|^2$ and $|\beta(t)|^2$, respectively.

For the case of $\delta \neq 0$, the upper-level populations go towards to zero in the long time limit. For example, if we consider the case in which $\delta >> \Gamma_1, \Gamma_2$, the exponential factors of the last terms of eqs. (2.14) and (2.15) can be ignored. Then, the equations leads to the exponentially decaying populations. On the other side, for the case of $\delta << 0.5\left(\Gamma_1 + \Gamma_2\right)$, it is shown in the Appendix-B that the real parts of $S_i - 0.5\gamma_j$ (i,j=1,2) are negative. When we evaluate the upper level population for the latter case, we also end-up with the exponentially decaying population.

In Fig. 2.2, we plot the upper level populations. The level $|2\rangle$ is initially empty. However, as time evolves, its population firstly increases and then tends to zero. On the other hand, the population of the level $|3\rangle$ tediously decreases to zero. Because the two

decay channels interfere so that the initially empty level increases before tending to zero (Zhu et al. (1995)).

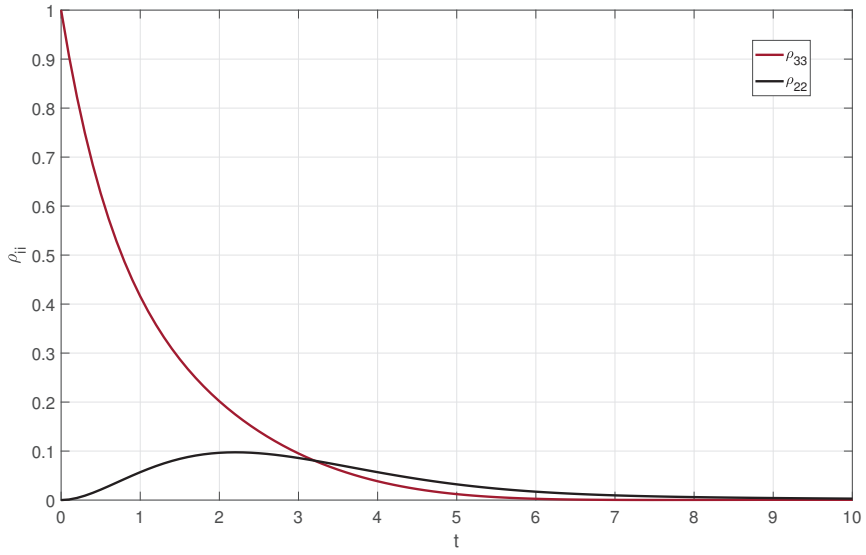

Figure 2.2. Upper level populations in time. Initially populated state is $|3\rangle$, and its population ρ_{33} (red curve) tediously tends to zero. The population of the level $|2\rangle$, ρ_{22} (black curve), which is initially empty first increases due to the transferred population from level $|3\rangle$, and then tends to zero. ($\delta = \Gamma_3$ and $\Gamma_2 = 0.5\Gamma_3$).

We also plot the population of the initially empty level $|2\rangle$ for some small values of δ. For all values of δ, population reaches a maximum value a little less than 0.25. These results are shown in Fig. 2.3 For example, for $\delta = 0.1\Gamma_3$, the maximum value is 0.244. It is also seen that as delta increases the maximum value of the population of the level $|2\rangle$ decreases.

The population in the initially empty level $|2\rangle$ oscillates in time for some situations. These oscillations tends to zero after several cycles. On the other hand, the population in the other upper level, level $|3\rangle$, is also oscillates. In Fig. 2.4 the population of the upper level $|2\rangle$ is plotted for $\delta = 5\Gamma_3$ and $\Gamma_3 = \Gamma_2$, it shows the oscillations of the population.

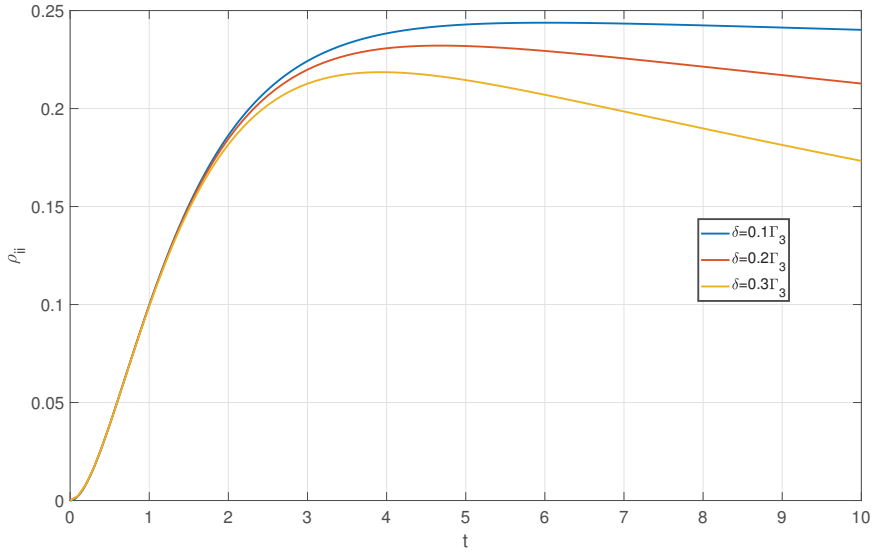

Figure 2.3. Maximum value of temporary population in level $|2\rangle$ for three different values of δ, $\delta = 0.1\Gamma_3$ (blue curve), $\delta = 0.2\Gamma_3$ (red curve), and $\delta = 0.3\Gamma_3$ (orange curve) ($\Gamma_3 = \Gamma_2$).

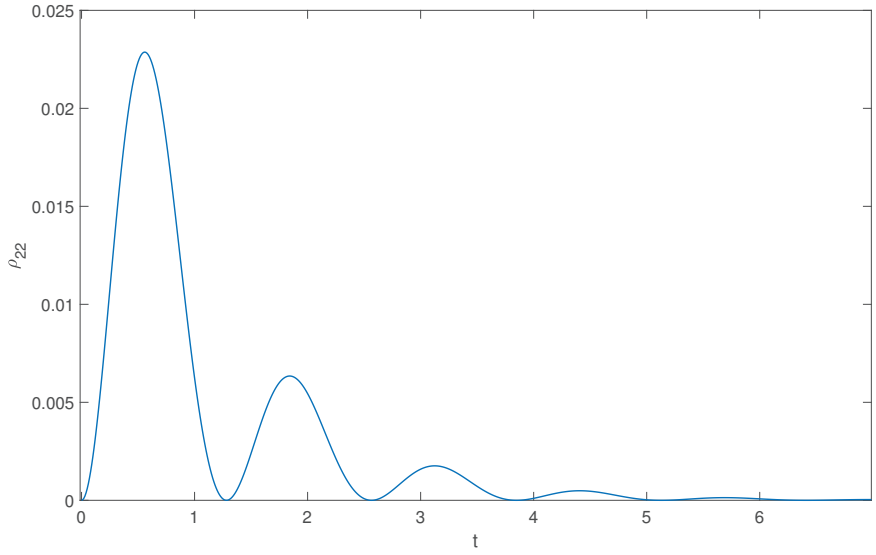

Figure 2.4. Illustration of the oscillation of the population in level $|2\rangle$ ($\delta = 5\Gamma_3$ and $\Gamma_2 = \Gamma_3$).

In order to see the dependence of the total population of the two upper levels to their frequency shift δ, we plot the total upper level populations as a function of time for different delta δ values with the same Γ_3 and Γ_2 values. Results are presented in the following figure. As seen in Fig. 2.5 the total population decay is not an exponential decay.

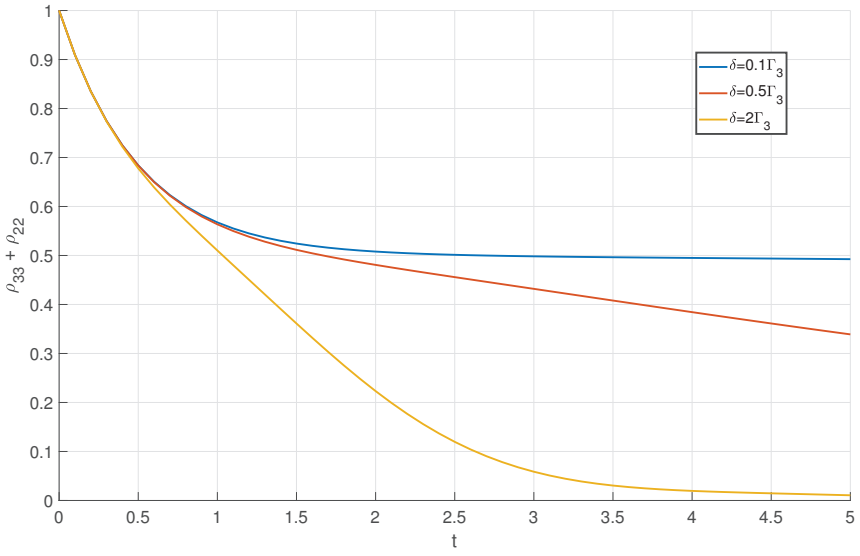

Figure 2.5. Total upper level population in time for a few different values of δ. $\delta = 0.1\Gamma_3$ (blue curve), $\delta = 0.5\Gamma_3$ (red curve), and $\delta = 2\Gamma_3$ (orange curve) ($\Gamma_3 = \Gamma_2$).

So far we have dealt with the non-zero frequency shift case (i.e. $\delta \neq 0$). Now, we examine the case for $\delta = 0$. In this case, the eqs. for the probability amplitudes become

$$\alpha(t) = C_1 + C_2 e^{S_2 t} e^{-\frac{\Gamma_2+\Gamma_3}{2}t} \tag{2.38}$$

$$\beta(t) = -\left(\frac{\Gamma_2}{\Gamma_3}\right)^{1/2} C_1 + \left(\frac{\Gamma_3}{\Gamma_2}\right)^{1/2} C_2 e^{S_2 t} e^{-\frac{\Gamma_2+\Gamma_3}{2}t} \tag{2.39}$$

If C_1 is not zero, upper level populations may not completely decay. In other words, some of the upper level populations may be trapped.

2.3. Power Spectrum of Emitted Light

The spectrum of the spontaneously emitted light by the atom is the Fourier transform of the following field correlation function (Narducci et al. (1990)):

$$\langle \hat{\mathbf{E}}^{-}(t+\tau)\hat{\mathbf{E}}^{+}(t)\rangle_{t\to\infty} = \langle\psi(t)| \sum_{k,k'} \hat{b}_k^{\dagger}(t)\hat{b}_k(t)e^{i\omega_k(t+\tau)}e^{-i\omega_{k'}t}|\psi(t)\rangle_{t\to\infty}. \tag{2.40}$$

By substituting the eq. (2.7) into (2.40), one can show that the spectrum is proportional to $|\gamma_k(\infty)|^2$, where $|\gamma_k(\infty)|$ is given by:

$$\gamma_k(\infty) = \frac{g_k^{(1)}C_1\left(1-2S_1/\Gamma_3\right)}{S_1 - 0.5\Gamma_3 - i(0.5\delta - \delta_k)} + \frac{g_k^{(1)}C_2\left(1-2S_2/\Gamma_3\right)}{S_2 - 0.5\Gamma_3 - i(0.5\delta - \delta_k)} \tag{2.41}$$

where δ_k is the detuning between the vacuum mode and the central frequency (from the middle point of the two upper levels to the lower level, as depicted in Fig. 2.6).

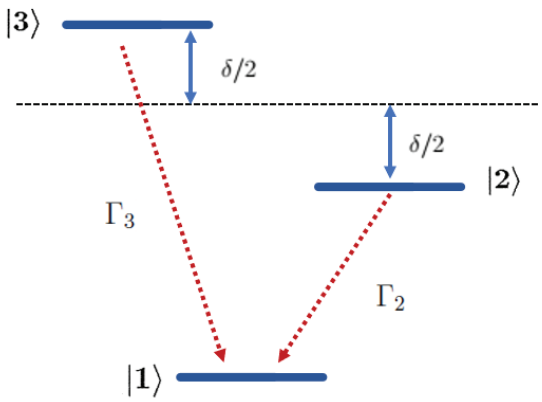

Figure 2.6. Schematic representation of the three-level atom considered in this section. The dashed black line is located at the middle of the energy difference of the upper levels. $\left(\delta_k = \omega_k - \frac{1}{2}\left(\omega_3 - \omega_2\right)\right)$.

One can obtain the spectrum by taking the absolute square of the eq. (2.41):

$$S(\omega_k) \propto |\gamma_k(\infty)|^2. \tag{2.42}$$

The spectrum of the spontaneously emitted light in the case of a two-level atom is a Lorentzian (Auffeves et al. (2008)) with a peak located at the atomic transition frequency. For the three-level atom, the population of the initially occupied level (level $|3\rangle$) partially passes to the other level (level $|2\rangle$). Due to the transferred population, the spectrum of the light for the three-level atom case is expected to be different from the two-level atom case. As the time evolves, the population in level $|2\rangle$ eventually decay to the lower level. Therefore, a major difference between the two types of spectrum, is the frequency components at the transition frequency from level $|2\rangle$ to $|1\rangle$. In Fig. 2.7, we plot the spontaneous emission spectrum for both the two-level atom and the three-level atom. It is easily seen that the weight of the transitions between level $|2\rangle$ and $|1\rangle$ is larger for the three-level atom case.

If the spectrum of the emitted light by the three-level atom is just the addition of the two spontaneous decay processes, it can be said that the spectrum consists of two peaks located at the two transition frequencies. However, the spectrum does not consist of the two-peaks located at the transition frequencies from the levels $|2\rangle$ and $|3\rangle$ to the level $|1\rangle$. Therefore, due to the strong interference between the two decay channels, the spectrum of the spontaneous emission from a three-level atom is not a two-peak distribution (Li et al. (2010)). In Fig. 2.7, it can be seen that the spectrum of the three-level atom (blue curve in Fig. 2.7) contains a dark line (Fano (1961), Zhu et al. (1995)). Indeed, one can show that $\gamma_k(\infty) = 0$ when the frequency of the emitted light ω_k is equal to the transition frequency from level $|2\rangle$ to $|1\rangle$, while the initially populated state is level $|3\rangle$.

Let us assume that the atom is initially in level $|3\rangle$, and we want to evaluate $B_k(\infty)$ at $\omega_k = \omega_2$ in this case $\delta_k = -0.5\delta$. By substituting $\delta_k = -0.5\delta$ into Eq. (2.41), we obtain

$$\gamma_k(\infty) = \frac{g_k^{(1)} C_1 \left(1 - 2S_1/\Gamma_3\right)}{S_1 - 0.5\Gamma_3 - i\delta} + \frac{g_k^{(1)} C_2 \left(1 - 2S_2/\Gamma_3\right)}{S_2 - 0.5\Gamma_3 - i\delta}, \tag{2.43}$$

and by using the following relations $S_1 S_2 = -\Gamma_3\Gamma_2/4$ and $S_1 + S_2 = 0.5\left(\Gamma_3 - \Gamma_2\right) + i\delta$

the Eq. (2.43) can be written as following:

$$\begin{aligned}\gamma_k(\infty) &= \frac{4g_k^{(1)}C_1S_1\left(-S_2-0.5\Gamma_2\right)/\Gamma_3\Gamma_2}{S_1-0.5\Gamma_3-i\delta} \\ &+ \frac{4g_k^{(1)}C_2S_2\left(-S_1-0.5\Gamma_2\right)/\Gamma_3\Gamma_2}{S_2-0.5\Gamma_3-i\delta} \\ &= \frac{4g_k^{(1)}\left(S_1C_1+S_2C_2\right)}{\Gamma_3\Gamma_2}.\end{aligned} \tag{2.44}$$

By inserting the initial conditions, $\alpha(0) = 1$ and $\beta(0) = 0$, into the Eqs. (2.34) and (2.35), one can see that $S_1C_1 + S_2C_2 = 0$ which yields $\gamma_k(\infty) = 0$. This tells us that at $\omega_k = \omega_2$ a dark line appears in the spectrum.

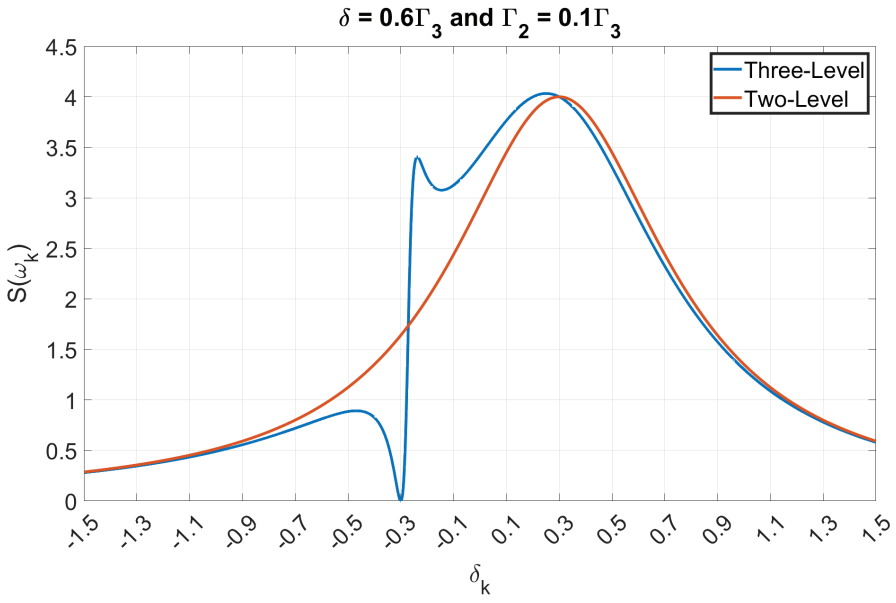

Figure 2.7. Spectrum of the light emitted spontaneously by a three-level atom (blue curve) for $\delta = 0.6\Gamma_3$, and $\Gamma_2 = 0.1\Gamma_3$, and by a two-level atom (red curve) with decay rate Γ_3.

The decay rate of the initially empty level, in our case the level $|2\rangle$, determines the width of the dark line. Thus, for an atom initially in the state $|3\rangle$ with the same Γ_3 and δ but different Γ_2, the spontaneous emission spectrum is plotted in Fig. 2.8. It is obvious

that as the decay rate of the initially empty level increases the width of the dark line also increases. If one of the decay rates Γ_3 or Γ_2 tends to zero the dark line will be narrower and narrower, and the spectrum becomes a Lorentzian.

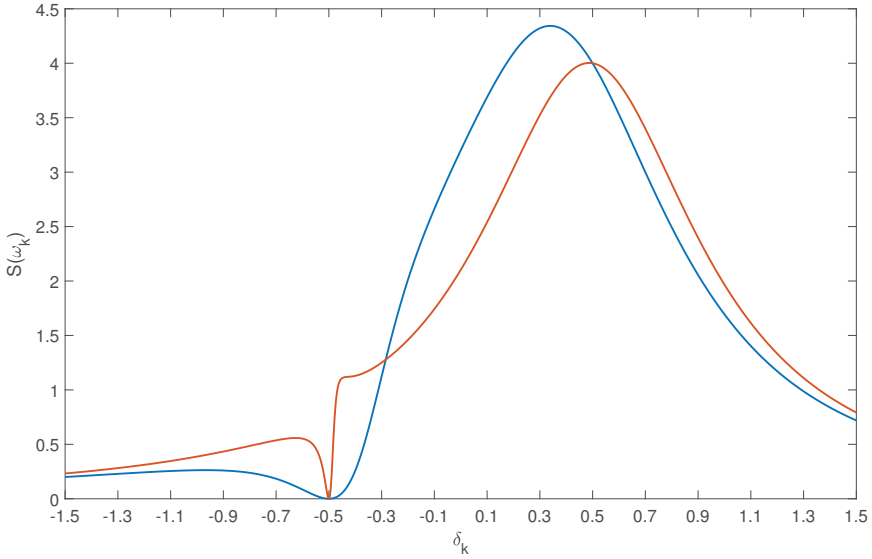

Figure 2.8. Dependence of the width of the dark line in the spontaneous emission spectrum of a three-level atom to the decay rate Γ_2. $\delta = \Gamma_3$, and $\Gamma_2 = 0.5\Gamma_3$ (blue curve), $\Gamma_2 = 0.05\Gamma_3$ (red curve).

As we mentioned previously that the decay rate of the corresponding upper level transition determines the width of the dark line. As the decay rate of the level increases, the width of the dark line increases too. In the previous example, we consider a decay rate for level $|2\rangle$, the state that determines the dark line width, so that the ratio Γ_2/Γ_3 much more smaller than 1. This is because to see a clear dark line. Instead, if we choose Γ_2 of the same order or even larger than Γ_3, the dark line width will be big enough to narrow the spectrum. In Fig. 2.9, the spectrum is plotted for three different values of the ratio Γ_2/Γ_3, and it is seen that as the ratio increases the width of the dark line increases at the same time the width of the spectrum becomes narrower as the ratio increases.

So far, we have assumed that the initially only one of the upper level is populated. In order to make a more comprehensive analysis, we present in Fig. 2.10, the results for some initial conditions corresponding an atom in a superposition of the upper-levels.

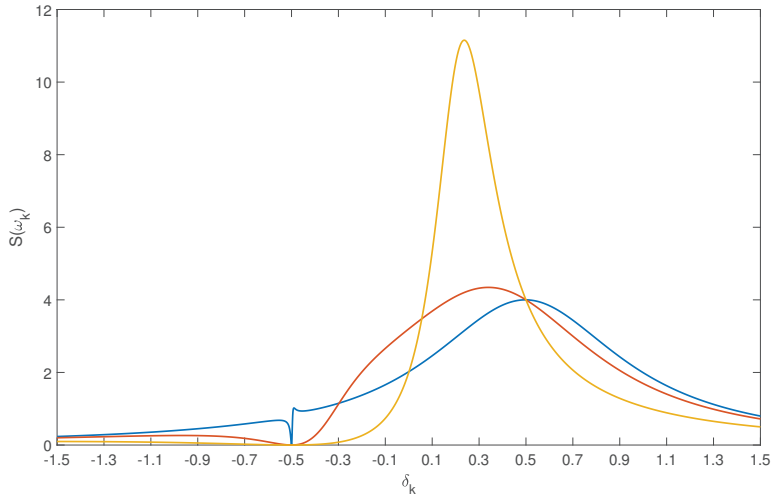

Figure 2.9. Narrowing of the spectrum by increasing the ratio Γ_2/Γ_3. Blue curve $(\Gamma_2/\Gamma_3 = 0.01)$, red curve $(\Gamma_2/\Gamma_3 = 0.5)$, orange curve $(\Gamma_2/\Gamma_3 = 2)$, and $\delta = \Gamma_3$.

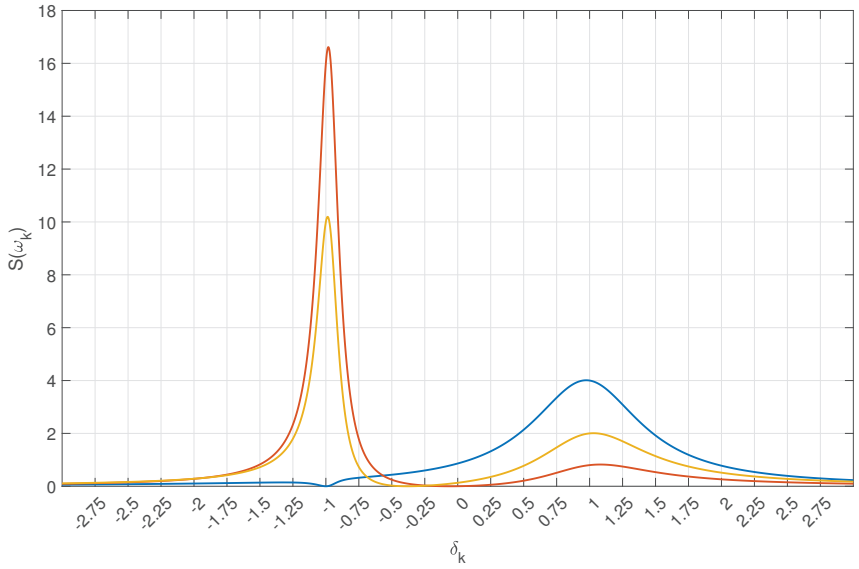

Figure 2.10. Spectrum of the emitted light for three different initial conditions: $\alpha(0) = 1, \beta(0) = 0$ (blue curve), $\alpha(0) = 0.5\beta(0)$ (red curve), and $\alpha(0) = \beta(0)$ (orange curve). $(\delta = 2\Gamma_3, \Gamma_2 = \Gamma_3)$.

CHAPTER 3

FLUORESCENCE SPECTRUM OF A TWO-LEVEL ATOM

In this chapter, we aim to evaluate the spectrum of the light that is scattered by a two-level atom driven by a monochramatic classical field. Here we have assumed an isolated atom that is constant in position. Thus, the relaxation of the atom to equilibrium with the driving field results from the coupling between the atom and the quantized electromagnetic modes into which the atom radiates (Mollow and Miller (1969)).

In this model, the contribution of the inelastically scattered light to the spectrum is shown. The source of the inelastic contribution is the alteration of the atomic energy levels by the driving field. However, in the weak driving limit case, the elastic component substantially dominates. The inelastic contribution appears as the driving field intensity increases. When the Rabi frequency Ω becomes comparable to the atomic decay rate, the inelastic components contribute significantly. In the limit that $\Omega >> \Gamma$, the inelastic components dominates over the elastic component. The spectrum has three peaks centred at the frequency ω of the driving field, and at the frequencies $\omega \pm \Omega$ of the displaced frequency of the field. The widths of these peaks are proportional to the atomic decay rate Γ. This spectrum famously known as the Mollow triplet which is theoretically described first by the B. R. Mollow in 1969 (Mollow (1969)). The Mollow triplet first observed in atomic beams.

3.1. Equations of Motion

In this case, we consider the model in which a two-level atom driven by a monochromatic classical field of the form

$$\mathbf{E}(t) = \mathbf{E}_0 cos(wt), \tag{3.1}$$

which oscillates near resonance with one of the atomic transition frequencies. In the dipole and the rotating-wave approximations, the coupling between the atom and the driving field is

$$\hat{H}_I = -\hat{\mathbf{d}}.\mathbf{E}(t) \tag{3.2}$$

$$= -\mathbf{d}.\mathbf{E}_0 \left(\hat{\sigma}_+ + \hat{\sigma}_-\right) cos(\omega t) \tag{3.3}$$

$$= -\frac{\mathbf{d}.\mathbf{E}_0}{2} \left(\hat{\sigma}_+ e^{-i\omega t} + \hat{\sigma}_- e^{i\omega t}\right), \tag{3.4}$$

and the Heisenberg picture Hamiltonian describing the system is given by

$$\hat{H} = \frac{1}{2}\hbar\omega_0\hat{\sigma}_3(t) + \sum_k \hbar\omega_k \hat{a}_k^\dagger(t)\hat{a}_k(t)$$
$$+ \hbar\sum_k g_k[\hat{\sigma}_+(t)\hat{a}_k(t) + \hat{a}_k^\dagger(t)\hat{\sigma}_-(t)] + \frac{\hbar\Omega}{2}\left[\hat{\sigma}_+(t)e^{-i\omega t} + \hat{\sigma}_-(t)e^{i\omega t}\right]. \tag{3.5}$$

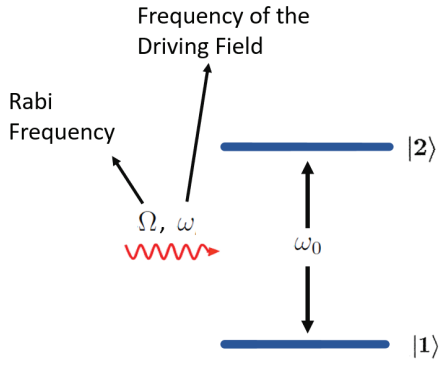

Figure 3.1. Schematic representation of the driven two-level atom. $|2\rangle$ corresponds to the state with higher energy, and ω_0 is the frequency difference between the states $|2\rangle$ and $|1\rangle$. Ω is the Rabi frequency (represents the frequency of the induced transitions) of the external driving field. ω is the frequency of the incident field.

Since, in the Heisenberg picture, the operators are time dependent (Sakurai and

Tuan (1994)), we write all the operators in the Hamiltonian in Eq. (3.5) in time dependent form. The g_k is the coupling strength, and Ω is the Rabi frequency, and they are given by the following expressions

$$g_k = -\mathbf{d}.\mathbf{e}_k \left(\frac{\hbar\omega_k}{2\epsilon_0 V}\right)^{1/2} \tag{3.6}$$

$$\Omega = -\frac{\mathbf{d}.\mathbf{E}_0}{\hbar}. \tag{3.7}$$

In order to get ride of the time dependent exponential factors in the last term of the above Hamiltonian, the transformation with $\hat{U} = exp\left(i\frac{\omega}{2}t\sigma_3\right)$ into an interaction picture introduces the time dependence $exp(iwt)$ in the third expression. To cancel this time dependence, a further transformation with $\hat{U} = exp\left(i\omega t\sum_k \hat{a}_k^\dagger \hat{a}_k\right)$ is made. The resulting Hamiltonian for this system is

$$\begin{aligned}\hat{\mathcal{V}} = &\frac{1}{2}\hbar\Delta\hat{\sigma}_3(t) + \sum_k \hbar\Delta_k \hat{a}_k^\dagger(t)\hat{a}_k(t) \\ &+ \hbar\sum_k g_k[\hat{\sigma}_+(t)\hat{a}_k(t) + \hat{a}_k^\dagger(t)\hat{\sigma}_-(t)] + \frac{\hbar\Omega}{2}\left[\hat{\sigma}_+(t) + \hat{\sigma}_-(t)\right],\end{aligned} \tag{3.8}$$

where $\Delta = \omega_0 - \omega$ and $\Delta_k = \omega_k - \omega$.

We proceed by writing the Heisenberg equations of motion for the atomic and the field operators. These are

$$\dot{\hat{\sigma}}_- = -i\Delta\hat{\sigma}_-(t) + i\sum_k \hbar g_k \hat{a}_k(t)\hat{\sigma}_3(t) + i\frac{\Omega}{2}\hat{\sigma}_3(t) \tag{3.9}$$

$$\dot{\hat{\sigma}}_+ = i\Delta\hat{\sigma}_+(t) - i\sum_k \hbar g_k \hat{a}_k^\dagger(t)\hat{\sigma}_3(t) - i\frac{\Omega}{2}\hat{\sigma}_3(t) \tag{3.10}$$

$$2\dot{\hat{\sigma}}_3 = -i\sum_k g_k\left[\hat{a}_k(t)\hat{\sigma}_+(t) - \hat{a}_k^\dagger(t)\hat{\sigma}_-(t)\right] - i\Omega\left[\hat{\sigma}_+(t) + \hat{\sigma}_-(t)\right] \tag{3.11}$$

$$\dot{\hat{a}}_k = -i\Delta_k\hat{a}_k(t) - ig_k\hat{\sigma}_-(t) \tag{3.12}$$

$$\dot{\hat{a}}_k^\dagger = i\Delta_k\hat{a}_k^\dagger(t) + ig_k\hat{\sigma}_+(t). \tag{3.13}$$

Now, formally integrating the eqs. (3.12) and (3.13), we have

$$\hat{a}_k(t) = e^{-i\Delta_k t}\hat{a}_k(0) - ig_k \int_0^t dt' e^{-i\Delta_k(t-t')}\hat{\sigma}_-(t') \tag{3.14}$$

$$\hat{a}_k^\dagger(t) = e^{i\Delta_k t}\hat{a}_k^\dagger(0) + ig_k \int_0^t dt' e^{i\Delta_k(t-t')}\hat{\sigma}_+(t') \tag{3.15}$$

and putting into (3.9) to (3.11) and making the Markov approximation will give the following Langevin equations

$$\dot{\hat{\sigma}}_- = -\left(\frac{\Gamma}{2} + i\Delta\right)\hat{\sigma}_-(t) - \hat{\sigma}_3(t)\hat{F}(t) + i\frac{\Omega}{2}\sigma_3(t) \tag{3.16}$$

$$\dot{\hat{\sigma}}_+ = -\left(\frac{\Gamma}{2} - i\Delta\right)\hat{\sigma}_+(t) - \hat{F}^\dagger(t)\hat{\sigma}_3(t) - i\frac{\Omega}{2}\sigma_3(t) \tag{3.17}$$

$$\dot{\hat{\sigma}}_3 = 2\left[\hat{\sigma}_+(t)\hat{F}(t) + \hat{F}^\dagger(t)\hat{\sigma}_-(t)\right] \tag{3.18}$$

$$-\Gamma\left[\hat{\sigma}_3(t) + 1\right] + i\Omega\left[\sigma_-(t) - \sigma_+(t)\right] \tag{3.19}$$

At this stage, we take the expectation values of the above operators. As mentioned previously in section 1.4, the decorrelation of the expectation values of the terms that include the multiplication of the atomic operator with the Langevin operator will throw away the influence of the temperature. However, we assume here that the temperature is zero so that we can decorrelate these terms which are exactly equal to zero. Thus, we obtain the equations of motion for the expectation values of the atomic operators as

$$\langle\dot{\hat{\sigma}}_-\rangle = \left(-\frac{\Gamma}{2} - i\Delta\right)\langle\hat{\sigma}_-(t)\rangle + i\frac{\Omega}{2}\langle\sigma_3(t)\rangle \tag{3.20}$$

$$\langle\dot{\hat{\sigma}}_+\rangle = \left(-\frac{\Gamma}{2} + i\Delta\right)\langle\hat{\sigma}_+(t)\rangle - i\frac{\Omega}{2}\langle\sigma_3(t)\rangle \tag{3.21}$$

$$\langle\dot{\hat{\sigma}}_3\rangle = -\Gamma\left[\langle\hat{\sigma}_3(t)\rangle + 1\right] + i\Omega\left[\langle\sigma_-(t)\rangle - \langle\sigma_+(t)\rangle\right]. \tag{3.22}$$

By using the relations

$$\hat{\sigma}_+ = \frac{1}{2}\left(\hat{\sigma}_x + i\hat{\sigma}_y\right) \tag{3.23}$$

$$\hat{\sigma}_- = \frac{1}{2}\left(\hat{\sigma}_x - i\hat{\sigma}_y\right), \tag{3.24}$$

we can write

$$\frac{d}{d\tau}\langle\hat{\sigma}_x(t+\tau)\hat{\sigma}_-(t)\rangle = -\frac{\Gamma}{2}\langle\hat{\sigma}_x(t+\tau)\hat{\sigma}_-(t)\rangle - \Delta\langle\hat{\sigma}_y(t+\tau)\hat{\sigma}_-(t)\rangle \tag{3.25}$$

$$\begin{aligned}\frac{d}{d\tau}\langle\hat{\sigma}_y(t+\tau)\hat{\sigma}_-(t)\rangle &= -\frac{\Gamma}{2}\langle\hat{\sigma}_y(t+\tau)\hat{\sigma}_-(t)\rangle \\ &\quad + \Delta\langle\hat{\sigma}_x(t+\tau)\hat{\sigma}_-(t)\rangle - \Omega\langle\hat{\sigma}_3(t+\tau)\hat{\sigma}_-(t)\rangle\end{aligned} \tag{3.26}$$

$$\begin{aligned}\frac{d}{d\tau}\langle\hat{\sigma}_3(t+\tau)\hat{\sigma}_-(t)\rangle &= -\Gamma\left[\langle\hat{\sigma}_3(t+\tau)\hat{\sigma}_-(t)\rangle + \langle\hat{\sigma}_-(t)\rangle\right] \\ &\quad + \Omega\langle\hat{\sigma}_y(t+\tau)\hat{\sigma}_-(t)\rangle.\end{aligned} \tag{3.27}$$

The above system of equations are called as the optical Bloch equations, and can be represented in the vector-matrix form as

$$\frac{d}{d\tau}\vec{C}(\tau) = \begin{bmatrix} -\frac{\Gamma}{2} & -\Delta & 0 \\ \Delta & -\frac{\Gamma}{2} & -\Omega \\ 0 & \Omega & -\Gamma \end{bmatrix}\vec{C}(\tau) + \vec{\alpha}_0 \tag{3.28}$$

where

$$\vec{C}(\tau) = \begin{bmatrix} \langle\hat{\sigma}_x(t+\tau)\hat{\sigma}_-(t)\rangle \\ \langle\hat{\sigma}_y(t+\tau)\hat{\sigma}_-(t)\rangle \\ \langle\hat{\sigma}_3(t+\tau)\hat{\sigma}_-(t)\rangle \end{bmatrix},\ \vec{\alpha}_0 = -\Gamma\begin{bmatrix} 0 \\ 0 \\ \langle\hat{\sigma}_-(t)\rangle \end{bmatrix}. \tag{3.29}$$

According to the assumption that the two-time correlation functions only depend on the τ at long times (Barnett and Radmore (1997)), we take $\tau = 0$. Therefore, this gives

the steady state values of the correlation functions as the initial conditions to the above system of differential equations. That is, at long times we have

$$\begin{bmatrix} \langle \hat{\sigma}_x(t+\tau)\hat{\sigma}_-(t)\rangle \\ \langle \hat{\sigma}_y(t+\tau)\hat{\sigma}_-(t)\rangle \\ \langle \hat{\sigma}_3(t+\tau)\hat{\sigma}_-(t)\rangle \end{bmatrix} \xrightarrow{\tau=0} \begin{bmatrix} \langle \hat{\sigma}_x(\infty)\hat{\sigma}_-(\infty)\rangle \\ \langle \hat{\sigma}_y(\infty)\hat{\sigma}_-(\infty)\rangle \\ \langle \hat{\sigma}_3(\infty)\hat{\sigma}_\infty(t)\rangle \end{bmatrix}. \tag{3.30}$$

Now we derive the steady state values of these correlation functions:

$$\begin{bmatrix} \langle \hat{\sigma}_x(\infty)\hat{\sigma}_-(\infty)\rangle \\ \langle \hat{\sigma}_y(\infty)\hat{\sigma}_-(\infty)\rangle \\ \langle \hat{\sigma}_3(\infty)\hat{\sigma}_-(\infty)\rangle \end{bmatrix} = \begin{bmatrix} \frac{1}{2}(\langle \hat{\sigma}_3(\infty)\rangle + 1) \\ \frac{-i}{2}(\langle \hat{\sigma}_3(\infty)\rangle + 1) \\ -\langle \hat{\sigma}_-(\infty)\rangle \end{bmatrix}. \tag{3.31}$$

As $t \to \infty$, the rate of change of the expectation values of the atomic operators is zero, then the eqs. (3.18) to (3.20) becomes

$$0 = \left(-\frac{\Gamma}{2} - i\Delta\right)\langle \hat{\sigma}_-(\infty)\rangle + i\frac{\Omega}{2}\langle \sigma_3(\infty)\rangle \tag{3.32}$$

$$0 = \left(-\frac{\Gamma}{2} + i\Delta\right)\langle \hat{\sigma}_+(\infty)\rangle - i\frac{\Omega}{2}\langle \sigma_3(\infty)\rangle \tag{3.33}$$

$$0 = -\Gamma\left[\langle \hat{\sigma}_3(\infty)\rangle + 1\right] + i\Omega\left[\langle \sigma_-(\infty)\rangle - \langle \sigma_+(\infty)\rangle\right]. \tag{3.34}$$

We solve these equations for $\langle \hat{\sigma}_3(\infty)\rangle$ and $\langle \hat{\sigma}_-(\infty)\rangle$, these are found to be

$$\langle \hat{\sigma}_-(\infty)\rangle = \frac{-i\Omega\left(\frac{\Gamma}{2} - i\Delta\right)}{\Omega^2 + \frac{\Gamma^2}{2} + \Delta^2} \tag{3.35}$$

$$\langle \hat{\sigma}_3(\infty)\rangle = \frac{\frac{-\Gamma^2}{2} - \Delta^2}{\Omega^2 + \frac{\Gamma^2}{2} + \Delta^2}. \tag{3.36}$$

Up to now, we write all the equations for non-zero detuning case (i.e. $\Delta \neq 0$). The analitical solution for this case is not included in this study. Instead, we present numerical solution for the case of non-zero detuning at the end of the next section. However, we solved the problem analitically for $\Delta = 0$.

3.2. Resonance Fluorescence

The emission of a resonantly excited two-level atom is known as the resonance fluorescence (Flagg et al. (2009), Field et al. (1975)). For the dressed atom description of the resonance fluorescence, the following reference might be useful (Cohen-Tannoudji and Reynaud (1977)).

We start by rewriting the optical Bloch equations which are written in the vector-matrix form, previously. In this case, for $\Delta = 0$, we have

$$\frac{d}{d\tau}\vec{C}(\tau) = \begin{bmatrix} -\frac{\Gamma}{2} & 0 & 0 \\ 0 & -\frac{\Gamma}{2} & -\Omega \\ 0 & \Omega & -\Gamma \end{bmatrix} \vec{C}(\tau) + \vec{\alpha_0}. \tag{3.37}$$

The solution to this system of non-homogeneous first order differential equations have a form given by the following expression

$$\vec{C}(\tau) = \sum_{i=1}^{3} c_i e^{\lambda_i \tau} |\vec{\lambda_i}\rangle + \vec{\alpha}, \tag{3.38}$$

where λ_i and $|\vec{\lambda_i}\rangle$ are the eigenvalues and the eigenvectors of the coefficient matrix, respectively. c_i's are the constants need to be determined from the initial conditions which are given by

$$\begin{bmatrix} \langle\hat{\sigma}_x(\infty)\hat{\sigma}_-(\infty)\rangle \\ \langle\hat{\sigma}_y(\infty)\hat{\sigma}_-(\infty)\rangle \\ \langle\hat{\sigma}_3(\infty)\hat{\sigma}_-(\infty)\rangle \end{bmatrix} = \begin{bmatrix} \frac{1}{2}(\langle\hat{\sigma}_3(\infty)\rangle + 1) \\ \frac{-i}{2}(\langle\hat{\sigma}_3(\infty)\rangle + 1) \\ -\langle\hat{\sigma}_-(\infty)\rangle \end{bmatrix}. \tag{3.39}$$

Here we have to write the expressions in eqs. (3.35) and (3.36) for the case of zero

detuning (i.e. $\Delta = 0$). They are

$$\langle \hat{\sigma}_-(\infty) \rangle = \frac{-i\Omega\frac{\Gamma}{2}}{\Omega^2 + \frac{\Gamma^2}{2}}, \tag{3.40}$$

$$\langle \hat{\sigma}_3(\infty) \rangle = \frac{\frac{-\Gamma^2}{2}}{\Omega^2 + \frac{\Gamma^2}{2}}. \tag{3.41}$$

Lastly, the vector $\vec{\alpha}$ is the particular solution given by

$$\vec{\alpha} = -A^{-1}\vec{\alpha}_0, \tag{3.42}$$

where A^{-1} is the inverse of the coefficient matrix. Then, the above expression becomes

$$\vec{\alpha} = \Gamma\langle \hat{\sigma}_-(t) \rangle \begin{bmatrix} 0 \\ \frac{2\Omega}{\Gamma^2+2\Omega^2} \\ \frac{-\Gamma}{\Gamma^2+2\Omega^2} \end{bmatrix}. \tag{3.43}$$

The eigenvalues of the coefficient matrix are found to be

$$\lambda_1 = -\frac{\Gamma}{2} \tag{3.44}$$

$$\lambda_{2,3} = -\frac{3}{4}\Gamma \pm \frac{1}{4}\sqrt{\Gamma^2 - 16\Omega^2}, \tag{3.45}$$

and the corresponding eigenvectors are

$$\vec{v}_1 = \begin{bmatrix} 1 \\ 0 \\ 0 \end{bmatrix}, \ \vec{v}_2 = \begin{bmatrix} 0 \\ \frac{\lambda_2+\Gamma}{\Omega} \\ 1 \end{bmatrix}, \vec{v}_3 = \begin{bmatrix} 0 \\ \frac{\lambda_3+\Gamma}{\Omega} \\ 1 \end{bmatrix}. \tag{3.46}$$

Now, we have to determine the constants c_i's by imposing the initial conditions. Let us start by writing the solution in an explicit form by also invoking the initial condi-

tions as

$$\begin{bmatrix} \frac{1}{2}(\langle\hat{\sigma}_3(\infty)\rangle + 1) \\ \frac{-i}{2}(\langle\hat{\sigma}_3(\infty)\rangle + 1) \\ -\langle\hat{\sigma}_-(\infty)\rangle \end{bmatrix} = c_1 \begin{bmatrix} 1 \\ 0 \\ 0 \end{bmatrix} + c_2 \begin{bmatrix} 0 \\ \frac{\lambda_2+\Gamma}{\Omega} \\ 1 \end{bmatrix} + c_3 \begin{bmatrix} 0 \\ \frac{\lambda_3+\Gamma}{\Omega} \\ 1 \end{bmatrix} + \begin{bmatrix} 0 \\ \frac{-2i\Gamma^2\Omega^2}{(\Gamma^2+2\Omega^2)^2} \\ \frac{i\Gamma^3\Omega}{(\Gamma^2+2\Omega^2)^2} \end{bmatrix}. \tag{3.47}$$

The above relation leads to the following system of equations

$$\frac{1}{2}\left[\langle\hat{\sigma}_3(\infty)\rangle + 1\right] = c_1 \tag{3.48}$$

$$-\frac{i}{2}\left[\langle\hat{\sigma}_3(\infty)\rangle + 1\right] = c_2\frac{(\lambda_2+\Gamma)}{\Omega} + c_3\frac{(\lambda_3+\Gamma)}{\Omega} - \frac{2i\Gamma^2\Omega^2}{\left(\Gamma^2+2\Omega^2\right)^2} \tag{3.49}$$

$$-\langle\hat{\sigma}_-(\infty)\rangle = c_2 + c_3 + \frac{i\Gamma^3\Omega}{\left(\Gamma^2+2\Omega^2\right)^2}. \tag{3.50}$$

By solving the eqs. (3.49) and (3.50), we obtain the following expressions for c_2 and c_3:

$$c_2 = \frac{i\Omega^3\left[\Gamma\sqrt{\Gamma^2-16\Omega^2}+\Gamma^2-4\Omega^2\right]}{\left(\Gamma^2+2\Omega^2\right)^2\sqrt{\Gamma^2-16\Omega^2}} \tag{3.51}$$

$$c_3 = \frac{i\Omega^3\left[\Gamma\sqrt{\Gamma^2-16\Omega^2}-\Gamma^2+4\Omega^2\right]}{\left(\Gamma^2+2\Omega^2\right)^2\sqrt{\Gamma^2-16\Omega^2}}. \tag{3.52}$$

Now,one can write the solution as following:

$$\begin{aligned} \vec{C}(\tau) &= \begin{bmatrix} \langle\hat{\sigma}_x(t+\tau)\hat{\sigma}_-(t)\rangle \\ \langle\hat{\sigma}_y(t+\tau)\hat{\sigma}_-(t)\rangle \\ \langle\hat{\sigma}_3(t+\tau)\hat{\sigma}_-(t)\rangle \end{bmatrix} \\ &= c_1e^{\lambda_1\tau}\begin{bmatrix} 1 \\ 0 \\ 0 \end{bmatrix} + c_2e^{\lambda_2\tau}\begin{bmatrix} 0 \\ \frac{\lambda_2+\Gamma}{\Omega} \\ 1 \end{bmatrix} + c_3e^{\lambda_3\tau}\begin{bmatrix} 0 \\ \frac{\lambda_3+\Gamma}{\Omega} \\ 1 \end{bmatrix} + \begin{bmatrix} 0 \\ \frac{\Gamma\langle\hat{\sigma}_-(t)\rangle 2\Omega}{\Gamma^2+2\Omega^2} \\ \frac{-\langle\hat{\sigma}_-(t)\rangle\Gamma^2}{\Gamma^2+2\Omega^2} \end{bmatrix}. \end{aligned} \tag{3.53}$$

By considering the relation in eq. (3.23), the two-time correlation function in the

steady-state can be written as

$$\langle\sigma_+(t+\tau)\sigma_-(t)\rangle_s = \frac{1}{2}\langle\sigma_x(t+\tau)\sigma_-(t)\rangle_s + \frac{i}{2}\langle\sigma_y(t+\tau)\sigma_-(t)\rangle_s, \tag{3.54}$$

the subscript s is used to indicate the steady-state values, where $\langle\sigma_x(t+\tau)\sigma_-(t)\rangle$ is given by the first row of the $\vec{C}(\tau)$ and $\langle\sigma_y(t+\tau)\sigma_-(t)\rangle$ is by the second row. By inserting the corresponding expressions into the (3.54), we can obtain the two-time correlation function in the limit as $t \to \infty$, which is

$$\begin{aligned}\langle\sigma_+(t+\tau)\sigma_-(t)\rangle_s = &\frac{1}{2}c_1 e^{\lambda_1\tau} \\ &+ \frac{i}{2}\left\{c_2 e^{\lambda_2\tau}\frac{(\lambda_2+\Gamma)}{\Omega} + c_3 e^{\lambda_3\tau}\frac{(\lambda_3+\Gamma)}{\Omega} + \frac{-2i\Gamma^2\Omega^2}{\left(\Gamma^2+2\Omega^2\right)^2}\right\},\end{aligned} \tag{3.55}$$

and then taking the Fourier transform of the two-time correlation function:

$$S(\omega) = 2Re\int_0^\infty \langle\sigma_+(t+\tau)\sigma_-(t)\rangle_s e^{-i\omega\tau}d\tau, \tag{3.56}$$

one can find the resonance fluorescence spectrum as

$$S(\omega) = \frac{2\pi\Gamma^2\Omega^2\delta(\omega)}{\left(\Omega^2+2\Gamma^2\right)^2} + \frac{\Gamma\Omega^2}{2\left(\Omega^2+2\Gamma^2\right)\left(\Gamma^2+4\omega^2\right)} - Re\sum_{j=2}^{3} i\frac{c_j\left(\lambda_j+\Gamma\right)}{\Omega\left(\lambda_j-i\omega\right)}. \tag{3.57}$$

The first term corresponds to the elastically scattered light which is centred on the atomic transition frequency in the case of resonance fluorescence. In Fig. 3.2, the contribution due to the other two terms is plotted. These correspond to the inelastic contributions. We plot the spectrum as a function of ω/Γ and the results shown are for the three distinct values of the Rabi frequency, for $\Omega = \Gamma, 3\Gamma$, and 9Γ. For small values of coupling strength, a single peak dominates as seen in the figure. As the Rabi frequency Ω increases, further two peaks slowly appear. For the large values of Ω, three nearly Lorentzian peaks show up. One of them is located at $\omega = 0$, and the symmetrically separated further two peaks are located at $\omega = \pm\Omega$.

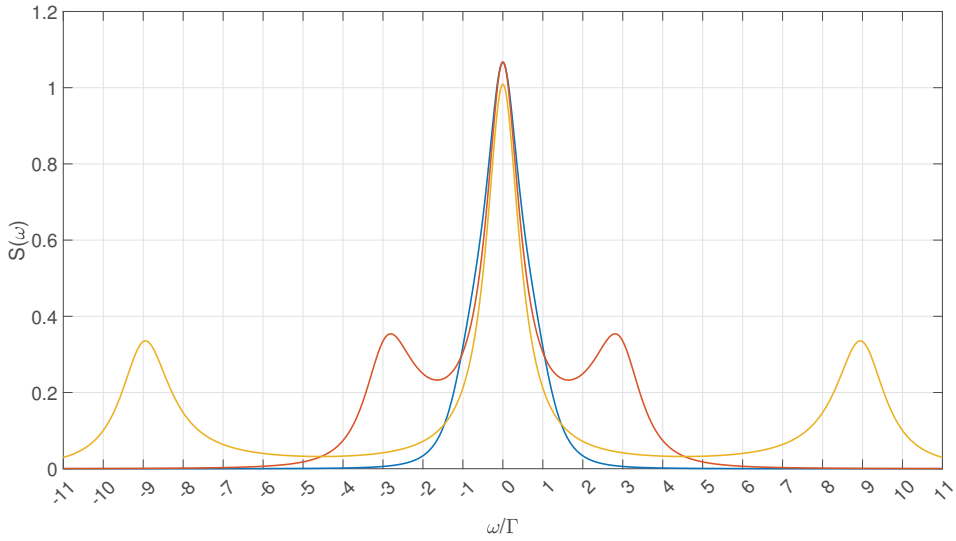

Figure 3.2. Resonance fluorescence spectrum of a two-level atom $(\Delta = 0)$. Weak coupling case: $\Omega = \Gamma$ (blue curve). Intermediate coupling case: $\Omega = 3\Gamma$ (red curve). Strong coupling case: $\Omega = 9\Gamma$ (orange curve).

3.3. Discussion and Results

In the last part of the previous section, the spectrum for the resonance case have been discussed. Now, we treat the problem by also including the weak coupling and the non-resonant cases. As we mentioned previously, for small values of the coupling strength (i.e. for values that are comparable to the decay rate Γ), we observe a single peak located at the atomic transition frequency, and as the coupling strength is increased side-bands begin to appear. In the following, the spectrum is plotted for different detuning Δ values for the case of weak coupling, i.e. $\Omega = 0.1\Gamma$, and for $\Omega = \Gamma, 5\Gamma$.

In Fig. 3.3, we plot the spectrum for $\Omega = 0.1\Gamma$ which corresponds to the weak coupling case. While keeping the coupling strength Ω constant, we change the detuning Δ in order to see the behaviour in the non-resonant excitation case. As it is expected, for $\Delta = 0$, the central peak dominates over the side-bands. The side-bands do not emerge in this case. As we increase the detuning, the central peak begins to shrink and at some value splits into two peaks. In our plot, this splitting is more noticeable for $\Delta = 0.6\Gamma$.

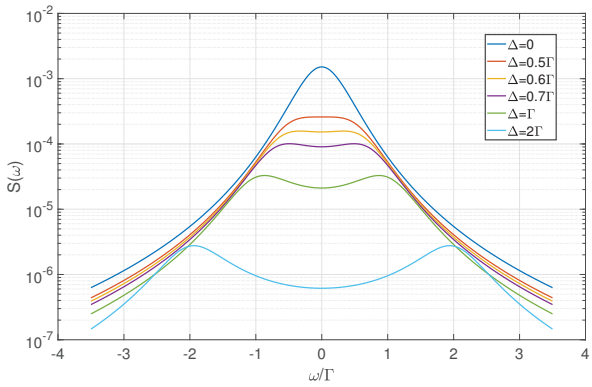

Figure 3.3. Fluorescence spectrum of a two-level system in the case of weak coupling and non-resonant excitation $(\Omega = 0.1\Gamma)$.

In the previous figure, Fig. 3.3, we considered the weak coupling case. Now, we plot, in Fig. 3.4, the spectrum for $\Omega = \Gamma$. As the coupling strength is increased, the contribution from the side-bands becomes apparent. After all, we do not see the contributions of the side-bands in the resonant excitation case. However, as the detuning is increased, the side-bands emerge. For $\Delta = 0.5\Gamma$, it can be seen that the curve tends to show the side-bands. At the same time, the central peak is suppressed as in Fig. 3.3. For example, for $\Delta = 2\Gamma$ the central peak is mostly suppressed, and the contributions of the side-peaks dominate.

In Fig. 3.5, we show a Mollow triplet series plotted for a constant excitation power (i.e. $\Omega = 5\Gamma$) with the variation of laser detuning Δ. As seen in Fig. 3.5, the side-bands always remain spectrally symmetric with respect to the center. The Rabi splitting increases with increasing detuning Δ (Ulhaq et al. (2012)).

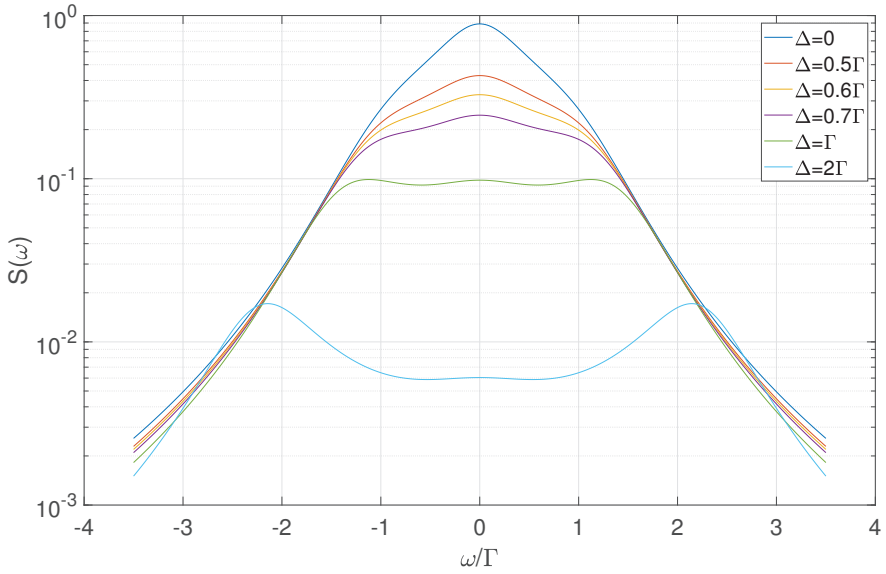

Figure 3.4. Fluorescence spectrum of a two-level atom for non-resonant and resonant cases ($\Omega = \Gamma$).

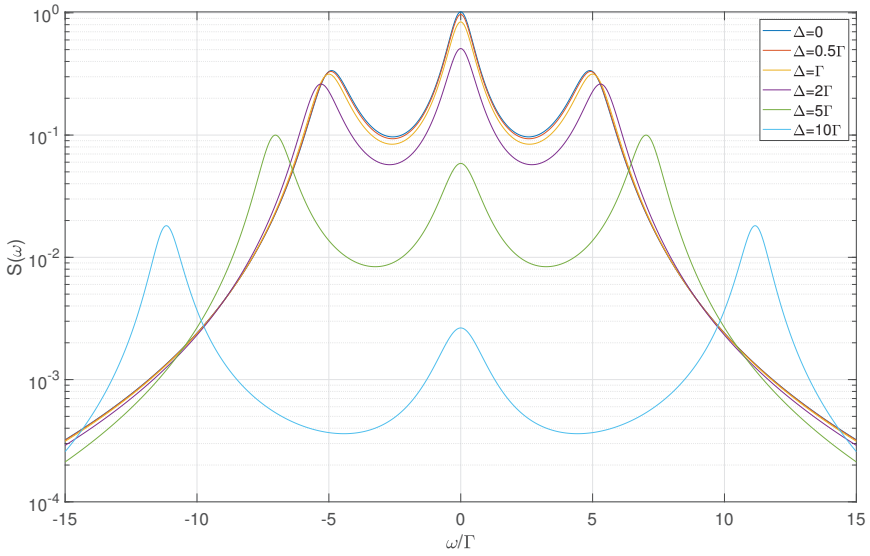

Figure 3.5. Fluorescence spectrum for a two-level atom in the strong coupling regime ($\Omega = 5\Gamma$), for the resonant $\Delta = 0$, and off-resonant $\Delta \neq 0$ cases.

CHAPTER 4

CONCLUSIONS

In the first part of this thesis, the spontaneous emission from a three-level atom with two-upper levels have investigated. The comparison to its counterpart of two-level atom is also included. In the three-level atom case, the additional upper level results in a dark line in the spontaneous emission spectrum due to the interference between the two decay processes. The decay rate of the additional upper level in the three level atom determines the width of the dark line. Larger decay rate results in wider dark lines, and the width of the central peak in the spectrum decreases as the dark line width increases.

In the second part, the fluorescence spectrum of a two-level atom driven on-resonance by a classical monochromatic field, and damped through the coupling to the quantized electromagnetic field modes has been evaluated in the strong coupling regime. The spectrum corresponds to the three peaks of inelastically scattered light which are located at the frequencies $\omega = 0$, and $\omega = \pm\Omega$ (Ω is the Rabi frequency). The elastically scattered light is attributed to the term which includes the delta-Dirac function and is discarded while plotting the spectrum since the elastic scattering is negligible for the strong coupling case. In order to see the effect of coupling for the resonance case, we plot the spectrum for three different values of coupling strength Ω. As the coupling strength increases, the side-peaks become more apparent and gets further away from the central peak. In the case of $\Omega = 9\Gamma$ which corresponds to the strong coupling regime, the widths of the side peaks are $3/2$ times the width of the central peak, and the heights of the side-peaks are one third of the central peak. On the other hand, in order to see the effect of detuning (i.e. the off-resonance condition), further three plots are included. In the weak coupling regime side-peaks are not apparent, and as the detuning increases the central peak shrinks and at some point begins to split into two peaks. For $\Delta = 2\Gamma$, these peaks almost completely disappear again. The splitting becomes more apparent for $\Delta = 0.6\Gamma$ in our plot, for the weak coupling case. However, side-peaks occur for $\Omega = \Delta$ as the detuning increases, and the central peak is suppressed.

REFERENCES

Auffeves, A., B. Besga, J. M. Gerard, and J. P. Poizat (2008, 6). Spontaneous emission spectrum of a two-level atom in a very-high- q cavity. *Physical Review A - Atomic, Molecular, and Optical Physics 77*.

Barnett, S. M. and P. M. Radmore (1997). (oxford series in optical and imaging sciences 15) stephen m. barnett, paul m. radmore - methods in theoretical quantum optics-clarendon press oxford university press (1997).

Boyanovsky, D. and D. Jasnow (2017, 12). Heisenberg-langevin versus quantum master equation. *Physical Review A 96*.

Breuer, H.-P. and F. Petruccione (1985). The theory of open quantum systems.

Cohen-Tannoudji, C. and S. Reynaud (1977). Dressed-atom description of resonance fluorescence and absorption spectra of a multi-level atom in an intense laser beam.

Fano, U. (1961). Effects of configuration interaction on intensities and phase shifts.

Field, M., F. Y. Wu, R. E. Grove, and S. Ezekiel (1975). Investigation of the spectrum of resonance fluorescence induced by a.

Flagg, E. B., A. Muller, J. W. Robertson, S. Founta, D. G. Deppe, M. Xiao, W. Ma, G. J. Salamo, and C. K. Shih (2009). Resonantly driven coherent oscillations in a solid-state quantum emitter. *Nature Physics 5*, 203–207.

Foerster, T. V. (1972, 6). Quantum theory of a damped two-level atom. *American Journal of Physics 40*, 854–862.

Gerry, C. and P. Knight (2004, 10). *Introductory Quantum Optics*. Cambridge University Press.

Iqbal, M. S., S. Mahmood, M. S. K. Razmi, and M. S. Zubairy (1988). Interaction of two two-level atoms with a single-mode quantized radiation field.

Irish, E. K. (2007, 10). Generalized rotating-wave approximation for arbitrarily large coupling. *Physical Review Letters 99*.

Jaynes, E. T. and F. W. Cummings (1963). Comparison of quantum and semiclassical radiation theories with application to the beam maser. *Proceedings of the IEEE 51*, 89–109.

Kobe, D. H. (1982, 2). Gauge transformations and the electric dipole approximation. *American Journal of Physics 50*, 128–133.

Li, Z. H., D. W. Wang, H. Zheng, S. Y. Zhu, and M. S. Zubairy (2010). Quantum interference due to energy shifts and its effect on spontaneous emission. *Physical Review A - Atomic, Molecular, and Optical Physics 82*.

Mollow, B. R. (1969). Power spectrum of light scattered by two-level systems.

Mollow, B. R. and M. M. Miller (1969). The damped driven two-level atom.

Narducci, L. M., M. O. Scully, G. L. Oppo, P. Ru, and J. R. Tredicce (1990). Spontaneous emission and absorption properties of a driven three-level system. *Physical Review A 42*, 1630–1649.

Pauli, W. (1980). Semiclassical theory of radiation.

Rzazewski, K. and R. W. Boyd (2004). Equivalence of interaction hamiltonians in the electric dipole approximation. *Journal of Modern Optics 51*, 1137–1147.

Sakurai, J. J. J. J. and S. F. Tuan (1994). *Modern quantum mechanics*. Addison-Wesley Pub. Co.

Shore, B. W. and P. L. Knight (1993). The jaynes cummings model. *Journal of Modern Optics 40*, 1195–1238.

Stenholm, S. and K.-A. Suominen (1930). Weisskopf-wigner decay of excited oscillator states.

Ulhaq, A., S. Weiler, S. M. Ulrich, R. RoÃbach, M. Jetter, and P. Michler (2012, 4). Cascaded single-photon emission from the mollow triplet sidebands of a quantum dot. *Nature Photonics 6*, 238–242.

Weisskopf, V. F. and E. Wigner (1930). Berechnung der nati rlichen linienbreite auf grund der dirac schen lichttheorie*.

Zhu, S.-Y., R. C. F. Chan, and C. P. Lee (1995). Spontaneous emission from a three-level atom.

Zhu, S.-Y., L. M. Narducci, and M. O. Scully (1995). Quantum-mechanical interference effects in the spontaneous-emission spectrum of a driven atom.

APPENDIX A

PRINCIPAL PART INTEGRALS

For a function $f(x)$ that does not have a finite limit at a point, say x_0, the integral $\int_a^b f(x)dx$ is not defined if x_0 is a point within the integration range. However, let us define the principal part integral as

$$P\int_a^b f(x)dx = \lim_{\delta\to 0}\left(\int_a^{x_0-\delta} f(x)dx + \int_{x_0+\delta}^b f(x)dx\right) \tag{A.1}$$

In most of the situations the limit gives a finite value. But, only the functions $f(x)$ behaving as $(x-x_0)^{-1}$ at $x = x_0$ will be considered here. Therefore, other way of expressing the principal part integral is

$$P\int_a^b f(x)dx = \lim_{\epsilon\to 0}\int_a^b \frac{(x-x_0)g(x)}{(x-x_0)^2+\epsilon^2}dx \tag{A.2}$$

where $f(x)$ is taken to be $g(x)/(x-x_0)$ and $g(x)$ is a finite function in the range of integration. In eq. (4.2), the limit must be taken after the integral is evaluated.

Now we take into account the integral I which is defined by the limit as ϵ tends to 0 from above. That is,

$$I = \lim_{\epsilon\to 0^+}\int_a^b \frac{g(x)}{i(x-x_0)+\epsilon}dx. \tag{A.3}$$

Separation of the real and imaginary parts of the integrand will yield

$$I = \lim_{\epsilon\to 0^+}\left(-i\int_a^b \frac{(x-x_0)g(x)}{(x-x_0)^2+\epsilon^2}dx + \pi\int_a^b \frac{(\epsilon/\pi)g(x)}{(x-x_0)^2+\epsilon^2}dx\right), \tag{A.4}$$

where the real part is the principal part integral given by eq. (4.2). The imaginary part go towards to the delta function $\delta(x-x_0)$ as the limit $\epsilon\to 0^+$. Thus, the integral becomes

$$I = -iP\int_a^b \frac{g(x)}{(x-x_0)}dx + \pi g(x_0). \tag{A.5}$$

Therefore, it can be written that

$$\lim_{\epsilon \to 0^+} \frac{1}{i(x - x_0) + \epsilon} = -i \frac{P}{x - x_0} + \pi \delta(x - x_0), \tag{A.6}$$

equality holds if the terms appear within an integral.